N-terminally truncated helper NLR *NRG1C* antagonizes immunity mediated by its full-length neighbors *NRG1A* and *NRG1B*

Zhongshou Wu[1,2], Lei Tian[1,2] and Xin Li[1,2*]

[1]Michael Smith Laboratories, University of British Columbia, Vancouver, BC V6T 1Z4, Canada

[2]Department of Botany, University of British Columbia, Vancouver, BC V6T 1Z4, Canada

*For correspondence: xinli@msl.ubc.ca

Short title: N-terminally truncated helper NLR NRG1C is functional

Abstract

Both animals and plants utilize nucleotide-binding leucine-rich repeat immune receptors (NLRs) to perceive the presence of pathogen-derived molecules and induce immune responses. *NLR* genes are far more abundant and diverse in higher plants. Interestingly, truncated NLRs, which lack one or more of the canonical domains, are also commonly encoded in plant genomes. However, little is known about their functions, especially regarding the N-terminally truncated ones. Here, we show that *Arabidopsis thaliana* (*A. thaliana*) N-terminally truncated helper NLR gene *NRG1C* (*N REQUIREMENT GENE 1*) is highly induced upon pathogen infection and in autoimmune mutants. The immune response and cell death conferred by some TIR (Toll/interleukin-1 receptor)-type NLRs (TNLs) are compromised in the *NRG1C* overexpression lines. Detailed genetic analysis revealed that NRG1C antagonizes the immunity mediated by its full-length neighbors *NRG1A* and *NRG1B*. Biochemical tests indicate that NRG1C possibly interferes with the EDS1-SAG101 complex, which likely signals together with NRG1A/1B. Interestingly, Brassicaceae NRG1Cs are functionally exchangeable, and the *Nicotiana benthamiana* (*N. benthamiana*) N-terminally truncated helper NLR NRG2 antagonizes NRG1 in tobacco. Together, our study uncovers an unexpected negative role of N-terminally truncated helper NLRs in different plants.

Keywords: NLR, N-terminally truncated NLRs, Helper NLRs, NRG1C, TNL, NLR cluster, Plant immunity, NRG1

Introduction

Plants utilize a sophisticated innate immune system to defend against a plethora of pathogens. They depend on immune receptors to recognize non-self and initiate defense. Plasma membrane localized pattern-recognition receptors (PRRs) can perceive pathogen-associated molecular patterns (PAMPs), leading to PAMP/pattern-triggered immunity (PTI) (Couto and Zipfel, 2016). On the other hand, intracellular nucleotide-binding leucine-rich repeat immune receptors (NLRs) are responsible for warding off adapted pathogens by detecting their secreted effectors, thereby activating effector-triggered immunity (ETI) (Cui et al., 2015).

NLRs are present in both animals and plants. They are members of the STAND (signal transduction ATPases with numerous domains) family consisting of a variable N-terminal domain, a central nucleotide-binding (NB) motif and a C-terminal leucine-rich repeat (LRR) region (Bonardi et al., 2012; Jones and Dangl, 2006). Typical plant sensor NLRs (sNLRs) have either a Toll/interleukin-1 Receptor (TIR) or a coiled-coil (CC) domain at their N-termini, and are termed TNLs (TIR-NB-LRR) or CNLs (CC-NB-LRR), respectively (Jones et al., 2016). They have evolved to recognize effectors directly or indirectly (Baggs et al., 2017). In contrast, a small subclass of NLRs is genetically required for diverse sNLRs' immune signaling. These NLRs are termed helper NLRs (hNLR) (Bonardi et al., 2011; Collier et al., 2011; Jubic et al., 2019; Peart et al., 2005). There are two *hNLR* gene families in *A. thaliana*, encoding RNLs (RPW8 (Resistance to Powdery Mildew 8) CC-NB-LRR): the *ACTIVATED DISEASE RESISTANCE 1* (*ADR1*) family (Bonardi et al., 2011) and the *N REQUIREMENGT GENE 1* (*NRG1*) family (Peart et al., 2005). Besides RNLs, the Solanaceae-specific CNL NRC (NB-LRR protein required for HR-associated cell death) proteins also function as hNLRs since both cell surface PRRs (Rathjen and Dodds, 2017; Wu et al., 2016) and many sNLRs signal through NRCs (Gabriëls et al., 2006; Gabriëls et al., 2007; Wu et al., 2017a). In comparison to the highly divergent sensor TNLs and CNLs, hNLRs are evolutionarily more conserved (Adachi et al., 2019; Andolfo et al., 2019; Shao et al., 2016; Wu et al., 2017a; Zhong and Cheng, 2016).

Plant *sNLRs* are among the most rapidly evolving genes (Gao et al., 2018; Guo et al., 2011; Van de Weyer et al., 2019). As a result, they are highly polymorphic. *NLR* allelic diversity mainly depends on the generation of either chimeric LRRs by intra- and intergenic recombination and gene conversion (Serra et al., 2018), or novel LRRs through point mutations (Lu et al., 2016; Mago et al., 2015; Michelmore and Meyers, 1998; Tamborski and Krasileva, 2020). Gene clustering is another feature commonly observed for plant *NLRs* (Van de Weyer et al., 2019). Two types of cluster patterns exist based on the diversity of *NLRs* within (Jacob et al., 2013). Homogenous clusters contain the same type of *NLRs* derived from tandem duplications. In contrast, heterogeneous clusters contain diverse *NLRs* generated by ectopic or large-scale segmental duplications (Jacob et al., 2013; Krasileva, 2019; Marone et al., 2013). Pan-genome analysis reveals that *NLR* cluster patterns vary among *A. thaliana* accessions. Some clusters have highly conserved copy numbers, while others show huge variations (Lee and Chae, 2020). An increasing number of examples suggest that clustered NLRs often are co-expressed and may cooperate to function. Clustering *sNLRs* together has the potential to massively expand pathogen recognition by increasing their oligomerization options (van Wersch and Li, 2019).

Duplication and uneven crossover events may generate *NLRs* lacking one or more of the canonical domains, yielding truncated *NLRs* (Baggs et al., 2017; Wicker et al., 2007), which are commonly found in all plant genomes (Bai et al., 2002; Jacob et al., 2013; Lee and Chae, 2020; Meyers et al., 2003; Meyers et al., 2002; Van de Weyer et al., 2019; Yang et al., 2008). Interesting, most truncated NLRs are expressed (Meyers et al., 2002; Nandety et al., 2013; Tan et al., 2007), suggesting their potential role in plant immunity. Several C-terminally truncated NLRs have been studied. For instance, *A. thaliana* TIR-only protein RBA1 (RESPONSE TO HOPBA1) is specifically required for defense responses mediated by bacterial effector HopBA1 (Nishimura et al., 2017). Another well-studied example includes the *A. thaliana* TN (TIR-NB) proteins CHS1 (CHILLING SENSITIVE 1) and TN2. CHS1 and TN2 form distinct pairs with full-length TNL SOC3 (SUPPRESSOR of *chs1-2*, 3) to monitor the homeostasis of E3 ligase SAUL1

(SENESCENCE-ASSOCIATED E3 UBIQUITIN LIAGASE 1) (Liang et al., 2019; Tong et al., 2017). However, little is known about the functions of N-terminally truncated NLRs, including NL (NB-LRR) and LRR proteins.

Although hNLRs may not have effector recognition capabilities, the NRG1-type *hNLRs* are organized in clusters in various plant species (Andolfo et al., 2019; Jubic et al., 2019; van Wersch and Li, 2019; Wu et al., 2019). In contrast, *ADR1s* are scattered in the genome (Bonardi et al., 2011; Dong et al., 2016). There are three *NRG1* paralogs in the *A. thaliana* genome: full length *NRG1A* and *NRG1B,* and N-terminally truncated *NRG1C* (Jubic et al., 2019; Wu et al., 2019). *NRG1A* and *NRG1B* are present in the *NRG1* cluster across almost all analyzed *A. thaliana* and *A. lyrate* accessions (Lee and Chae, 2020). *NRC1C* encodes a predicted protein missing the RPW8 CC domain and most of the NB domain. Similarly, *N. benthamiana* contains a copy of the full-length *NRG1* and an N-terminally truncated *NRG2*. In comparison to the clustered *NRG1s* in *A. thaliana*, *NRG2* does not cluster with *NRG1* and has been assumed to be a pseudogene (Peart et al., 2005). It is unclear whether these N-terminally truncated hNLRs have any biological roles.

Here, we describe the functional analysis of truncated hNLRs. To our surprise, NRG1C negatively regulates TNL autoimmune mutant *chs3-2D* (*chilling sensitive 3, 2D*)-mediated autoimmunity, serving an opposite role from its full-length paralogs NRG1A/1B. *NRG1C* overexpression plants phenocopy those of the *nrg1a nrg1b* double mutant or the *sag101* (*SENESCENCE-ASSOCIATED GENE 101*) single mutant. Biochemical analysis indicates that NRG1C possibly works by interfering with the EDS1 (ENHANCED DISEASE SUSCEPTIBILITY 1)-SAG101 complex. Interestingly, Brassicaceae NRG1Cs from different species are functionally exchangeable. In addition, the *N. benthamiana* truncated NRG2 also antagonizes NRG1-mediated cell death. In summary, our study uncovers an unexpected role of N-terminally truncated hNLRs, which was likely evolved to balance the activities of their corresponding full-length hNLRs.

131

Results

NRG1C is evolutionarily conserved in Brassicaceae and its expression is highly induced in TNL-type autoimmune mutants and upon pathogen infection

BLASTp analysis revealed that NRG1C (AT5G66890)-type N-terminally truncated hNLRs are present in all 8 well-sequenced Brassicaceae species and *N. benthamiana* (Figure 1A-B and Supplemental Figure 1). Additionally, *NRG1C* is present in most *A. thaliana* accessions. However, no NRG1C ortholog was found in available protein databases of other land plants. Interestingly, as with *A. thaliana NRG1C*, other Brassicaceae *NRG1C* orthologs also tend to cluster with the full length *NRG1* genes in their genomes (Supplemental Table 1). Phylogenetic analysis indicates that all Brassicaceae NRG1Cs came from the same ancestor (Figure 1B). The Brassicaceae *NRG1C* genes likely originated from either an initial gene duplication from the *NRG1A/1B* ancestor and a subsequent N-terminal loss, or partial gene duplication. In contrast, NbNRG2 and NbNRG1 belong to a distinct clade from Brassicaceae NRG1, suggestive of an independent evolution of NbNRG1 (Figure 1B and Supplemental Figure 1). In *Brassica rapa*, there are two close NRG1C homologs found in two separate gene clusters. Brara.I00877.1 and Brara.G01211.1 share 75.4% and 62.0% amino acid identity, or 86.2% and 75.5% similarity with NRG1C, respectively (Supplemental Figure 1). However, phylogenetic analysis indicates that Brara.G01211.1 might not be an NRG1C ortholog as it contains a full-length NB domain (Supplemental Figure 1) and is evolutionarily separate from the NRG1C clade (Figure 1B).

DAR5 (AT5G66630, DA1-RELATED PROTEIN 5) was proposed to be a chimeric protein resulting from a translocation of NRG1C and a fusion with a member of the nearby cluster carrying DAR homologs, DAR7 (AT5G66610) to DAR3 (AT5G66640) (Meyers et al., 2003). Coincidently, DAR5 carries RPW8, NB and LIM (Lin11, Isl-1 & Mec-3) domains, but no LRRs. It shares high similarity with NRG1s in *A. thaliana* (Andolfo et al., 2019; Castel et al., 2019). However, DAR5 seems to be unique in *A.*

thaliana, as BLAST searches failed to identify putative DAR5 orthologs in genomes of all other sequenced plant species.

To test whether the truncated *NRG1C* and *DAR5* are involved in TNL-mediated immunity, their expression levels were first measured in TNL autoimmune mutants. *snc1* (*suppressor of npr1-1, constitutive 1*) and *chs3-2D* contain gain-of-function mutations in the *TNLs SNC1* and *CHS3*, respectively, resulting in TNL-mediated autoimmunity. *NRG1C* transcripts were around 200 and 7000-fold up-regulated respectively in *snc1* and *chs3-2D* mutants as compared with that of Col-0 wild-type (WT) (Figure 1C). However, no significant *DAR5* transcript changes were observed (Figure 1D). Furthermore, the transcript of *NRG1C*, but not *DAR5*, was highly induced in WT plants upon infection by virulent bacterial pathogen *Pseudomonas syringae* pv. *maculicola* (*P.s.m.*) ES4326 (Figure 1E). These expression analyses suggest that *NRG1C* in the *NRG1* gene cluster may play roles in plant biotic responses against pathogens.

NRG1C, but not _DAR5_, negatively regulates _chs3-2D_ and _snc1_-mediated autoimmunity

As *NRG1C* is up-regulated in autoimmune mutants and during infection, and the *nrg1c* knockout does not seem to exhibit severe immune related defects and affect *snc1* autoimmunity (Wu et al., 2019), we used an overexpression approach to examine the role of these truncated NLRs. *NRG1C* and *DAR5* were individually overexpressed in *chs3-2D* and *snc1* backgrounds. To our surprise, overexpression of *NRG1C* fully suppressed *chs3-2D*-mediated dwarfism (Figure 2A-C) and enhanced disease resistance to the oomycete pathogen *Hyaloperonospora arabidopsidis* (*H.a.*) Noco2 (Figure 2D). In contrast, no suppression of *chs3-2D*-mediated growth defects was observed upon *DAR5* overexpression (Supplemental Figure 2A-B). Furthermore, overexpressing *NRG1C* (Figure 2E) could partially suppress *snc1*-mediated dwarfism to a similar level as the *NRG1* deletion mutant (Wu et al., 2019) (Figure 2F-G). Consistently, enhanced disease resistance to *H.a.* Noco2 (Figure 2H) and *P.s.t.* DC3000 (Figure 2I) in *snc1* were partially suppressed upon *NRG1C* overexpression. However, the *snc1 DAR5 OE* lines did not

show significant differences in growth compared with *snc1* (Supplemental Figure 2C-D). Taken together, NRG1C negatively regulates *chs3-2D* and *snc1*-mediated autoimmunity with different strengths. Intriguingly, these phenotypes closely resemble those of the *nrg1a nrg1b* double mutant and the *sag101* single mutant (Wu et al., 2019; Xu et al., 2015).

ADR1-L3 is dispensable for *snc1*-mediated autoimmunity and RPP4-mediated immunity

Similar to NRG1C in the NRG1 family, the *A. thaliana* ADR1 helper NLR family includes a truncated ADR1-L3, missing the N-terminal RPW8 domain (Supplemental Figure 3). In contrast to the broad presence of NRG1C in Brassicaceae, an ADR1-L3 ortholog is only found in *Boechera stricta* (Supplemental Figure 3). To test whether ADR1-L3 is involved in immunity conferred by ADR1-dependent NLRs, *ADR1-L3* was overexpressed in *snc1* background. As shown in Supplemental Figure 4A-B, *snc1*-mediated growth defects (Supplemental Figure 4A) and enhanced disease resistance (Supplemental Figure 4B) were not altered upon *ADR1-L3* overexpression. Furthermore, *ADR1-L3* overexpression lines in WT were not susceptible to oomycete pathogen *H.a.* Emwa1 (Supplemental Figure 4C), which is recognized by ADR1-dependent TNL RPP4 (*RECOGNITION OF PERONOSPORA PARASITICA 4*) (Bonardi et al., 2011; Dong et al., 2016). Taken together, unlike NRG1C, ADR1-L3 does not seem to play any roles in TNL-mediated autoimmunity and defense.

Overexpression of *NRG1C* has no effect on *chs1-2*- and *chs2-1*-mediated autoimmunity, RPS2 and RPS4-mediated immunity, or basal defense

To further test the specificity of NRG1C, *NRG1C* was overexpressed in additional autoimmune mutants. In *chs1-2* (*chilling sensitive 1*, *2*), a missense mutation in a truncated TN protein (Wang et al., 2013) results in constitutive cell death and defense responses at low temperatures (Zbierzak et al., 2013). Another chilling sensitive mutant *chs2-1* contains a gain-of-function mutation in the TNL *RPP4* (Huang et al., 2010).

However, neither *chs1-2* nor *chs2-1*-mediated temperature-dependent autoimmunity was suppressed upon *NRG1C* overexpression (Supplemental Figure 5A-B). Consistently, oomycete pathogen *H.a.* Emwa1 failed to grow in *NRG1C OE* lines in the WT background (Supplemental Figure 5C-D).

We also challenged two independent *NRG1C OE* lines (in WT Col-0 background) with *P.s.t.* DC3000 expressing either AvrRps4 or AvrRpt2 effectors, which are recognized by TNL RPS4 (RESISTANT TO *P. SYRINGAE* 4) or CNL RPS2 (RESISTANT TO *P. SYRINGAE* 2), respectively. However, no altered disease resistance against these avirulent pathogens was detected (Supplemental Figure 6A-B). When challenged with *P.s.t.* DC3000, *NRG1C OE* lines exhibited similar bacterial growth as WT, suggesting that overexpression of *NRG1C* does not compromise basal defense response either (Supplemental Figure 6C). Therefore, NRG1C seems to be specific to TNL-mediated immune response with unequal strengths for distinct TNLs. The differential contributions of NRG1C in TNL signaling are reminiscent of the phenotypes of *nrg1a nrg1b* or *sag101* knockouts, which play major roles in *chs3-2D* but relatively mild roles in *snc1*, but no roles in *chs1-2*, *chs2-1*, RPS4 and RPS2-mediated autoimmunity and bacterial growth (Castel et al., 2019; Feys et al., 2005; Wu et al., 2019; Xu et al., 2015).

NRG1C is required for HopQ1-1-mediated defense

NbNRG1 is essential for immune signaling triggered by effector HopQ1-1 (Qi et al., 2018). As *P.s.t.* DC3000 carries diverse effectors that can mask the effects of HopQ1-1, *P.s.t.* CUCPB5500 in which all 18 of the well-expressed T3SS (Type III secretion system) effectors were deleted, was used as a background to avoid interference from other effectors (Kvitko et al., 2009). When challenged with *P.s.t.* CUCPB5500, no bacterial growth difference was observed between *NRG1C OE* lines, *nrg1a nrg1b* double or *sag101-1* mutants as compared with WT (Figure 3A). However, WT exhibited enhanced disease resistance to *P.s.t.* CUCPB5500 expressing HopQ1-1, suggesting that unidentified R proteins can likely recognize HopQ1-1 in *A. thaliana*. Consistently with the observation in tobacco, this bacterial growth inhibition was largely compromised in

NRG1C OE lines, *nrg1a nrg1b* double mutant and *sag101* single mutant to a similar level (Figure 3A). Taken together, NRG1C antagonizes HopQ1-1-mediated defense responses in *A. thaliana*. *NRG1C* overexpression phenotypes seem identical to those of the *nrg1a nrg1b* double and the *sag101* single mutants.

NRG1C antagonizes AvrRPS4-mediated hypersensitive response

AvrRPS4 can activate RRS1 (RESISTANT TO RALSTONIA SOLANACEARUM 1)/RPS4 pairs, resulting in hypersensitive response (HR) in Col-0 background (Saucet et al., 2015). This HR is compromised in Col-0 *nrg1a nrg1b* double mutant, although no difference in *P.s.t.* AvrRPS4 bacterial growth can be observed (Supplemental Figure 6A) (Castel et al., 2019; Lapin et al., 2019). We thus tested whether NRG1C regulates RRS1/RPS4-mediated HR. Effector AvrRPS4 was delivered using *P. fluorescens* strain *Pf0-1* containing type III secretion system (*Pf0-1* EtHAn), but lacking type III effector genes (Thomas et al., 2009). Similar with the phenotype of *nrg1a nrg1b* double mutant (Castel et al., 2019; Lapin et al., 2019), RRS1/RPS4-mediated HR is lost in *NRG1C OE* lines (Figure 3B-C). The striking overall phenotypic resemblance between *NRG1C OE* lines and the *nrg1a nrg1b* double mutant indicates that NRG1C might function antagonistically with NRG1A/1B in *A. thaliana* to regulate defense responses.

NRG1C antagonizes the NRG1-SAG101 module, in parallel with the ADR1-PAD4 module

The similar phenotypes of *adr1 triple* with *pad4* (Phytoalexin deficient 4) mutants (Dong et al., 2016), and the additive effects between SAG101 and PAD4 (Rietz et al., 2011) or NRG1s and ADR1s (Lapin et al., 2019; Saile et al., 2020; Wu et al., 2019) allude to an EDS1-ADR1-PAD4 signaling module that works in parallel with an EDS1-NRG1-SAG101 module to regulate downstream events in TNL immunity. To test this further, higher order mutant combining loss-of-function mutations from different modules were generated in *snc1* background. The dwarfism and increased *PR1* (*Pathogenesis-Related 1*) gene expression of *snc1* was partially suppressed by introducing mutations in *SAG101*

(Feys et al., 2005) or *NRG1* cluster (Wu et al., 2019) (Figure 4A-B). However, *snc1 sag101-1 nrg triple* resembled the *snc1 sag101-1* and *snc1 nrg triple* in morphology (Figure 4A) and *PR1* gene expression levels (Figure 4B), confirming that SAG101 works in the same pathway as NRG1A/1B. In contrast, the increased *PR1* gene expression of *snc1* was largely, but not fully, suppressed by *adr1 triple* or *pad4-1* (Figure 4B), although the size of *snc1 adr1 triple* and *snc1 pad4-1* was WT like (Cheng et al., 2011; Dong et al., 2016) (Figure 4A). However, combining *adr1 triple* and *pad4* mutations together did not further reduce the *PR1* gene expression (Figure 4B and Supplemental Figure 7), confirming that ADR1s and PAD4 work in the same pathway. In contrast, mutants containing mutations in two components from different modules, including *snc1 pad4-c1 sag101-1*, *snc1 pad4-c1 nrg triple*, *snc1 sag101-c1 adr1 triple*, *snc1 adr1 triple nrg triple*, exhibited fully restored WT-like levels of *PR1* expression (Figure 4A-B and Supplemental Figure 7). Taken together, these epistasis analyses data confirm that two distinct modules are present in TNL pathways that act in parallel, one includes PAD4-ADR1s and the other includes SAG101-NRG1A/1B.

To examine the relationship between NRG1C and the NRG1-SAG101 module, *NRG1C* was overexpressed in the *snc1 nrg triple* or *snc1 sag101-1* background. As shown in Figure 4C, the dwarfism was not further suppressed by *NRG1C* overexpression. In agreement, *snc1 sag101-1 NRG1C OE* and *snc1 nrg triple NRG1C OE* resembled the *snc1 sag101-1* and *snc1 nrg triple* in regards to *PR1* gene expression (Supplemental Figure 8A). Specifically, the increased *PR1* gene expression in *snc1* was reduced by either *nrg triple* or *sag101*, but not further by *NRG1C* overexpression (Supplemental Figure 8A). In contrast, the partial suppression of up-regulated *PR1* gene expression in *snc1* by *adr1 triple* or *pad4-1* was further suppressed to WT levels when *NRG1C* was overexpressed in *snc1 adr1 triple* or *snc1 pad4-1* backgrounds (Supplemental Figure 8B). These comprehensive epistasis data support that NRG1C indeed specifically antagonizes the NRG1-SAG101 module.

NRG1C does not impact _NRG1A/1B_ through transcriptional interference

As *NRG1C* encodes a truncated hNLR and works antagonistically with the SAG101-NRG1 module, we first hypothesized that it might interfere with *NRG1A/1B* transcription through RNA-mediated interference due to their sequence similarity. To test this, *NRG1C* with a premature stop codon at position 213 of the predicted *NRG1C* mRNA sequence was overexpressed in *chs3-2D* background. Such a mutation would yield a non-functional protein NRG1C^{T71*} but a rather normal transcript. No alterations in *chs3-2D*-mediated dwarfism (Figure 5A-C) and enhanced disease resistance to *H.a.* Noco2 (Figure 5D) were observed by overexpression of *NRG1C^{T71*}* (Figure 5B), suggesting that NRG1C does not affect mRNA levels of the full-length helper *NRG1A/1B*. Thus, if NRG1C interferes with NRG1A/1B, the effects are likely protein-related.

NRG1C antagonizes NRG1A-mediated HR

To further examine the hypothesis that NRG1C might directly interfere with NRG1A/1B, we co-expressed *NRG1C* with the *NRG1A D485V*, an auto-active version of NRG1A that triggers HR in *N. benthamiana* (Wu et al., 2019). As shown in Supplemental Figure 9A-B, NRG1A D485V-triggered HR in *N. benthamiana* was alleviated when co-expressed with NRG1C, although the same amount of NRG1A D485V proteins accumulated (Supplemental Figure 9C). However, overexpression of *NRG1C* did not alter the autoimmunity of *ADR1-L2 D484V*, an auto-active variant of ADR1-L2 (Roberts et al., 2013) (Supplemental Figure 10A-C). Taken together, these data indicate that NRG1A-mediated HR are negatively regulated by NRG1C and the effects of NRG1C seem to be specific to NRG1-type hNLR-mediated defense responses.

NRG1C does not associate with full-length NRG1A

Since NRG1C does not affect the mRNA or protein levels of full-length NRG1A, another hypothesis is that NRG1C might interfere with NRG1A/1B through protein-protein interactions. The recently developed TurboID-based proximity labeling method allows TurboID-fused protein to biotinylate proximal and interacting proteins in the presence of biotin *in vivo* (Zhang et al., 2019). This unbiased method can more reliably detect weak

and transient protein-protein interactions. When NRG1A-HA-TurboID was co-expressed with NRG1C-3FLAG in the presence of RBA1, which induces NRG1 dependent immunity (Supplemental Figure 11A) (Qi et al., 2018; Wan et al., 2019), biotinylated NRG1C-3FLAG was not detected despite the fact that NRG1C-3FLAG protein was significantly enriched (Supplemental Figure 11B). This negative interaction result suggests that the NRG1C-mediated negative regulation of NRG1A-mediated defense may not be through direct protein interference. However, we cannot exclude the possibility that the *in planta* interactions between the two proteins could not be detected due to low protein expression or complex conformation constraints.

NRG1C associates with the EDS1-SAG101 complex

As *NRG1C* overexpression also shares similar phenotypes with the *sag101* knockouts, we then tested whether NRG1C could interfere with NRG1A-mediated defense by associating with SAG101 or its constitutively associated partner EDS1. When *N. benthamiana* leaves were infiltrated with *Agrobacterium* expressing EDS1-HA-TurboID, NRG1C-3FLAG and SAG101-3FLAG, both IP-enriched SAG101-3FLAG and NRG1C-3FLAG were biotinylated (Supplemental Figure 12A). This suggests that basal levels of NRG1C proteins are in close proximity to the C-terminus of EDS1, where the TurboID was fused. In comparison, in *N. benthamiana* leaves pre-infiltrated with *Agrobacterium* harboring RBA1, a similar amount of IP-enriched SAG101-3FLAG, but relatively more NRG1C-3FLAG, was biotinylated by EDS1-HA-TurboID (Figure 6D, Supplemental Figure 12A and 14C), suggesting that TNL activation likely enhances the association between NRG1C and the EDS1-SAG101 complex. Interestingly, when this TurboID-mediated proximity labeling assay was performed in the absence of SAG101-3FLAG, biotinylated NRG1C was no longer detected (Supplemental Figure 12B), indicating that the association between EDS1 and SAG101 is needed to retain NRG1C in the complex.

We further examined such interaction with a reciprocal TurboID-based proximity labeling assay using *A. thaliana* stable transgenic lines carrying both *NRG1C-HA-TurboID* and *SAG101-3FLAG*. Transgenic plants were pretreated with *Agrobacterium*

expressing RBA1 and whole seedling plants were harvested at 6 hpi. As shown in Figure 6E, although NRG1C-HA-TurboID could not be observed in the SAG101-3FLAG pull-down likely due to its low protein abundance, NRG1C-HA-TurboID successfully biotinylated SAG101-3FLAG, but not EDS1, even though a large amount of EDS1 protein was pulled down. This suggests that SAG101 is in close proximity with the C-terminus of NRG1C, where TurboID is fused. In addition, neither EDS1 (Supplemental Figure 13A-B) nor SAG101 (Supplemental Figure 13C-D) protein levels were altered by *NRG1C* overexpression, confirming that NRG1C does not affect the protein levels of the EDS1-SAG101-NRG1A/1B module.

TIR domains of many TNLs exhibit nicotinamide adenine dinucleotide (NAD^+) hydrolase (NADase) activity, with a conserved catalytic glutamic acid (Horsefield et al., 2019; Wan et al., 2019). The catalytically dead $RBA1_{E86A}$ mutant retains self-association, but fails to trigger cell death *in planta* (Wan et al., 2019). To test whether the association between NRG1C and the EDS1-SAG101 complex is influenced by the TIR NADase activity, *N. benthamiana* leaves expressing EDS1-HA-TurboID, SAG101-3FLAG and NRG1C-3FLAG were pretreated with *Agrobacterium* expressing $RBA1_{E86A}$ mutant. As shown in Supplemental Figure 14A and 14C, SAG101-3FLAG and basal levels of NRG1C-3FLAG were biotinylated by EDS1-HA-TurboID, suggesting that TIR NADase enzyme activity is required for TNL-enhanced high order complex formation.

As EDS1 also constitutively interacts with PAD4, we also tested whether NRG1C associates with the EDS1-PAD4 complex. However, when *N. benthamiana* leaves were infiltrated with *Agrobacterium* expressing EDS1-HA-TurboID, NRG1C-3FLAG and PAD4-ZZ-TEV-FLAG in the presence of RBA1 induction, EDS1-HA-TurboID was able to label PAD4-ZZ-TEV-FLAG, but not NRG1C-3FLAG (Supplemental Figure 14B). This specificity of NRG1C with SAG101 explains why NRG1C explicitly antagonizes EDS1-SAG101-NRG1 module-dependent immunity. It is worth noting that *N. benthamiana* contains its own copies of *NRG1*, *SAG101* and *EDS1*. NbSAG101 is apparently not sufficient to induce proximity between AtEDS1 and AtNRG1C (Supplemental Figure 12B and 14B). This is consistent with previous findings that lipase-

like proteins (EDS1, PAD4, and SAG101) and hNLRs (ADR1s and NRG1s) can only signal together when they come from the same species (Lapin et al., 2019).

Overexpression of *B. rapa* NRG1C ortholog suppresses *chs3-2D*-mediated defense

As the presence of *NRG1C*-type N-terminally truncated hNLRs in *NRG1* clusters seems to be a singular event in the evolution of Brassicaceae, we further tested whether they are functionally transferable among different Brassicaceae species. To test this, *Brara.I00877.1* (*BraNRG1C*) was overexpressed in the *chs3-2D* mutant. Consistent with the phylogeny that Brassicaceae NRG1C family arose from a common ancestor (Figure 1A), overexpression of *BraNRG1C* fully rescued the *chs3-2D*-mediated dwarfism (Figure 7A-C) and enhanced disease resistance to *H.a.* Noco2 (Figure 7D). Taken together, NRG1C function seems to be conserved in Brassicaceae species.

NbNRG2 negatively regulates HopQ1-1-mediated immunity in *N. benthamiana*

To further explore the function of truncated NRG1C outside the Brassicaceae, we examined *N. benthamiana* NRG2 (NbNRG2) in HopQ1-1-mediated NRG1-dependent ROQ1 (RECOGNITION of XopQ 1) resistance (Qi et al., 2018; Schultink et al., 2017) (Supplemental Figure 15A). Interestingly, overexpression of *NbNRG2* (Supplemental Figure 15B) could suppress HopQ1-1-mediated HR, which was induced by *P.s.t.* CUCPB5500 HopQ1-1 (Figure 7E and G). By contrast, the HopQ1-1-mediated HR was not suppressed by overexpression of Brassicaceae orthologs including *A. thaliana NRG1C* (Figure 7F and H; Supplemental Figure 15C) or *BraNRG1C* (Supplemental Figure 15D-F), indicating that these Brassicaceae orthologs are not able to inhibit *N. benthamiana* TNL ROQ1-mediated immunity. Furthermore, overexpression of *NbNRG2* (Supplemental Figure 16B) failed to suppress *chs3-2D*-mediated dwarfism (Supplemental Figure 16A and C) and enhanced disease resistance to *H.a.* Noco2 (Supplemental Figure 16D). Since molecular incompatibility among different species or clades was observed in the EDS1-SAG101-NRG1 module (Lapin et al., 2019), it is not surprising that NbNRG2

440 and Brassicaceae NRG1Cs are not functionally exchangeable and their negative
441 regulation requires molecular compatibility.
442
443

Discussion

Truncated NLRs, including TIR only, TN, TIR-unknown domain (TX), CC only, CC-NB (CN), CC-unknown domain (CX), RPW8 only, RPW8-NB (RN), NB-LRR (NL), NB only and LRR only, are commonly found encoded in the genomes of higher plants (Baggs et al., 2017; Bai et al., 2002; Jacob et al., 2013; Lee and Chae, 2020; Meyers et al., 2003; Meyers et al., 2002; Nandety et al., 2013; Van de Weyer et al., 2019; Yang et al., 2008). A genome-wide survey of *A. thaliana* NLR genes revealed that around 31% of NLR genes are truncated (Meyers et al., 2003). Among them, approximately 90% lack canonical C-terminal domains (Meyers et al., 2003; Meyers et al., 2002). Functional characterizations of some C-terminally truncated NLRs have been reported. The TIR-only protein RBA1 can function as an effector sensor and trigger plant immune responses by self-oligomerization (Nishimura et al., 2017). Moreover, the TIR domain in the RBA1 protein possesses NADase activity, which is required to trigger cell death (Wan et al., 2019). Other well-studied TN proteins include TN2 and CHS1. TN2 guards the exocyst complex subunit EXO70B1 (Zhao et al., 2015) and may stabilize active calcium-dependent protein kinase CPK5 to regulate defense responses (Liu et al., 2017). Interestingly, *TNL SOC3* and *CHS1* cluster together with *TN2* (Liang et al., 2019; Zhang et al., 2017). SOC3 pairs with either CHS1 or TN2 to monitor the absence or overaccumulation of E3 ligase SAUL1 (Liang et al., 2019; Tong et al., 2017). A recent study found that LRR-PL (Post-LRR) truncated protein $DM10^{TueScha-9}$ (DANGEROUS MIX 10) shows an incompatible interaction with $DM11^{Cdm-0}$ (DANGEROUS MIX 11), resulting in hybrid necrosis (Barragan et al., 2020). Therefore, the C-terminally truncated NLRs often can still serve positive roles in NLR activation, as they retain the N-terminal signaling domains such as the TIR and NB regions.

In contrast, about 10% of truncated NLRs are N-terminally truncated in *A. thaliana* (Meyers et al., 2003). Although they are widely present in all higher plant genomes, little is known about their biological significance. In mammalian system, the TLR (Toll-like receptors) TIR truncations can act as dominant-negative (DN) proteins to dampen immune responses by associating with the same immune activation complexes (Burns et

al., 2003; Padmanabhan et al., 2009; Wells et al., 2006). Here, similar to the truncated TLRs, the N-terminally truncated helper NRG1C lacking the RPW8 CC and part of the NB domain can negatively regulate NRG1A/1B-mediated defense responses. Compared to the DN-TLR examples in the mammalian system, how exactly NRG1C interferes with NRG1A/1B signaling is less clear. As overexpression of a *NRG1C* variant containing a premature stop codon failed to suppress *chs3-2D*-mediated autoimmunity, the mechanism is unlikely to be due to transcriptional interference (Figure 5). Additionally, NRG1A-HA-TurboID was unable to label NRG1C-3FLAG even in the presence of an elicitor, suggesting that NRG1C does not interact with NRG1A/1B, although caution should always be taken with negative protein-protein interaction data. However, NRG1C is in close proximity with the EDS1-SAG101 complex, and this association seems to be enhanced with TNL-induction (Figure 6A-B, Supplemental Figure 12A-B and 14C). To our delight, our observation was recently independently supported by a SAG101-YFP IP-MS (Immunoprecipitation Mass-Spectrometry) analysis, where peptides of NRG1C were abundantly observed in immuno-precipitates of SAG101-YFP upon *Pf0-1 avrRPS4* treatment (Figure 3a and Figure s5a, Sun et al., 2020). More peptides from NRG1C were present in the SAG101 IP than the ones from NRG1A/1B, corroborating the interaction between NRG1C and EDS1-SAG101. Additionally, Sun *et al.,* also found that NRG1A associates with the EDS1-SAG101 dimer in an effector-dependent manner. Although EDS1 is required for all tested TNLs, the SAG101-NRG1 branch plays unequal roles in different cases (Feys et al., 2005; Wu et al., 2019; Xu et al., 2015) For example, SAG101 and NRG1A/1B are fully required for *chs3-2D*-mediated autoimmunity, but they are not needed for CHS1-SOC3 or RPP4-mediated autoimmunity in *saul1-1* or *chs2-1* (Wu et al., 2019). Therefore, the EDS1-SAG101 dimer is specifically required for some, but not all TNLs-mediated immunity and NRG1C likely antagonizes NRG1A/1B signaling by interfering with the EDS1-SAG101 dimer. It seems that upon infection, a large complex consisting of EDS1, NRG1A/1B and SAG101 forms, and NRG1C likely acts by interfering with such complex assembly to avoid aberrant activation (Figure 7I). NRG1C may occupy the NRG1A/1B space in the EDS1-SAG101-NRG1 complex, preventing NRG1A/1B interaction with the lipase-like proteins. This explains the negative

interaction data between NRG1A and NRG1C. Further biochemical and structural analyses of these proteins are needed to clarify the details of these interactions.

Both NRG1C and ADR1-L3 are N-terminally truncated hNLRs. Although NRG1C negatively regulates some TNL-mediated defense, no effect on ADR1-dependent TNL mediated autoimmunity or pathogen growth was observed upon *ADR1-L3* overexpression (Supplemental Figure 4A-C). In contrast to NRG1C, ADR1-L3 retains the full NB domain (Supplemental Figure 1 and 3). NRG1C orthologs are commonly found in Brassicaceae (Figure 1A), whereas ADR1-L3 ortholog is only present in *Boechera stricta* (Supplemental Figure 3). Such an evolutionary difference indicates that ADR1-L3 is likely a pseudogene and thus was lost during evolution. Therefore, for N-terminally truncated NLRs in higher plant genomes, some may be pseudogenes, and some may have negative functions as with NRG1C. Although an evolutionary examination may provide an initial hint, functional analysis is needed to determine their exact roles.

Besides NRG1C and ADR1-L3, five additional N-terminally truncated *NB-LRR* genes are present in the *A. thaliana* Col-0 genome (Supplemental Table 2). AT4G19050, AT5G45510 and AT1G61300 are more closely related to CNLs (Meyers et al., 2003). *AT4G19050* is adjacent to a CN gene *AT4G19060*. *AT5G45510* and head-to-head arranged CNL *AT5G45520* form a cluster with two other CN genes *AT5G45490* and *AT5G45440*. *AT1G61310* and adjacent CNL *AT1G61300*, are transcribed in the same direction (Supplemental Table 2). Only two NL proteins, AT5G38350 and AT4G09360, share a similar NB motif with TNLs. *AT5G38350* clusters together with TIR-only gene *AT5G38344* and TNL gene *AT5G38340*, while *AT4G09360* resides in the TNL cluster containing TNL *AT4G09430* and *AT4G09420* (Supplemental Table 2). Therefore, clustering of *NL* genes with full-length or C-terminally truncated sNLRs can also be detected in *A. thaliana*. It is possible that the *NL* genes in these clusters plays a similar role as *NRG1C* in the *NRG1* cluster, serving negative regulatory functions. Additional investigations into the functions of such *NL* genes in *A. thaliana* and other plants will be of great interest to widen our understanding of NLRs.

535

536 **Materials and Methods**

537 **Plant growth conditions**

538 *A. thaliana* and *N. benthamiana* plants were grown at 22ºC under 16hr light/8hr dark
539 regime, unless otherwise specified. Severe autoimmune mutants were grown at 28 ºC to
540 suppress the dwarfism and enable seed production.

541 **Construction of plasmids**

542 Overexpression construct of *NRG1C* was made in *pCambia1305* vector. *NRG1C*^{T71*} was
543 cloned into *pCambia1305* vector as well. The overexpression construct of *NRG1C* in
544 *NRG1A D485V* was cloned into *pBASTA* vector. The overexpression constructs of
545 *BraNRG1C* and *NbNRG2* were cloned into *pBASTA* vector by using the extracted
546 genomic DNA from *Brassica napus L.* cv. *Westar* and *N. benthamiana*. *DAR5* was
547 cloned into *pHan* vector. For the TurboID-based proximity labeling assay, *NRG1A* and
548 *EDS1* were cloned into *pBASTA-HA-TurboID*. *NRG1C* was cloned into *pCambia1305-*
549 *3FLAG*. *pBASTA NRG1A-3FLAG* and *pCambia1300 EDS1-3FLAG* were described in
550 previous studies (Wu et al., 2019).

551 To generate the CRISPR/Cas9 constructs for knocking out *PAD4* and *SAG101*, genomic
552 sequences of *PAD4* and *SAG101* were subjected to CRISPRscan
553 (http://www.crisprscan.org/?page=sequence) to identify the target sequences. The
554 selected sequences were evaluated with Cas-OFFinder (http://www.rgenome.net/cas-
555 offinder/). The pHEE401E vector was used to generate the CRISPR/Cas9 constructs
556 following the protocols previously described (Wang et al., 2015). All primers used are
557 listed in Supplemental Table 3.

558 ***A. thaliana* stable transformation**

559 The binary constructs were introduced into *Agrobacterium tumefaciens* GV3101 by
560 electroporation and subsequently transformed into *A. thaliana* by the floral dipping
561 method (Clough and Bent, 1998). For *snc1*, *chs1-2* and *chs2-1* transformation, plants
562 were grown at room temperature. For *chs3-2D* transformation, plants were grown at 28ºC

563 under 16hr light/8hr dark regime to reduce autoimmunity. Transformants were selected
564 either on soil by spraying BASTA (Glufosinate ammonium) or on plates with
565 Hygromycin B. 10 transformants were selected each and co-segregation analysis in T2
566 generations were carried out to make sure the suppression phenotypes were due to the
567 transgene overexpression.

568 **Transient *N. benthamiana* expression**

569 Transient *N. benthamiana* expression assays were performed as previously described
570 (Wu et al., 2017b). In brief, *Agrobacteria* carrying the respective constructs were co-
571 infiltrated into four-week-old *N. benthamiana* leaves. Final OD_{600} for most strains was
572 0.2, whereas OD_{600} =1.0 and 0.6 were used for all strains expressing NRG1C or SAG101,
573 respectively. Each infiltration contained *Agrobacteria* expressing *p19* to inhibit gene
574 silencing (Lakatos et al., 2004).

575 **Pathogen infections**

576 Oomycete and bacterial pathogen infection assays were carried out as described
577 previously (Li et al., 2001). In brief, two-week-old soil-grown seedlings were sprayed
578 with *H.a.* Noco2 or Emwa1 conidia spores at a concentration of 10^5 spores per ml water.
579 Sporulation was quantified using a hemocytometer after plants were grown at 18°C for 7
580 days. For bacterial infections, four-week-old plants were infiltrated with bacterial
581 solution at designated concentrations. Leaf discs were collected and ground on the day of
582 infection (Day 0) and 3 days later (Day 3). Colony-forming units (cfu) were calculated
583 after incubation on LB plates with appropriate antibiotic selection. For HR assay in *A.*
584 *thaliana*, four-week-old soil-grown plants were hand infiltrated with *Pf0-1* carrying
585 pBS46:AvrRPS4. Cell death was monitored at 36 hpi.

586 **Expression analysis**

587 About 0.05 g of four-week-old soil-grown plant tissue was collected, and RNA was
588 extracted using an RNA isolation kit (Bio Basic; Cat#BS82314). ProtoScript II reverse
589 transcriptase (NEB; Cat#B0368) was used to generate cDNA. Real-time PCR was
590 performed using a SYBR premix kit (TaKaRa, Cat#RR82LR). The primers used are
591 listed in Supplemental Table 3.

592 ***Agrobacteria* infiltration following *P.s.t.* CUCPB5500 HopQ1-1 infection**

593 *Agrobacteria* carrying the respective constructs were infiltrated into four-week-old *N.*
594 *benthamiana* leaves. *P.s.t.* CUCPB5500 HopQ1-1 was then infiltrated in the indicated
595 area 48 hrs after *Agrobacteria* infiltration. Ion leakage was measured at 4 days after *P.s.t.*
596 CUCPB5500 HopQ1-1 infection.

597 **Ion leakage measurement in *N. benthamiana***

598 After agrobacteria infiltration and *P.s.t.* CUCPB5500 HopQ1-1 infection, leaf discs from
599 *N. benthamiana* were collected and washed in 10 ml of milliQ water overnight at room
600 temperature. Ion leakage was measured with a conductometer VWR E C METER Model
601 2052. All samples were then autoclaved to measure the total ion leakage.

602 **TurboID-based proximity labeling in *N. benthamiana***

603 TurboID-based proximity labeling assay was performed as described previously (Wu et
604 al., 2020; Zhang et al., 2019). In brief, *N. benthamiana* leaves were infiltrated with
605 agrobacteria containing *HA-TurboID* and *3FLAG* tagged constructs. At 48 hpi,
606 agrobacteria expressing RBA1 or $RBA1_{E86A}$ constructs were infiltrated (Wan et al., 2019).
607 At 52 hpi, biotin was infiltrated, and the plants were incubated at room temperature for 2
608 h to allow labeling. Leaves were harvested, followed by immunoprecipitation and
609 western blot analysis.

610 **TurboID-based proximity labeling in *Arabidopsis***

611 Two-week-old plate-grown *Arabidopsis* transgenic lines carrying both *NRG1C-HA-*
612 *TurboID* and *SAG101-3FLAG* were soaked with *Agrobacteria* expressing RBA1
613 (OD_{600}=0.2). At 4 hpi, biotin was added in solution and the plants were incubated at room
614 temperature for 2 hours for labeling. The plants were then harvested, followed by
615 immunoprecipitation and western blot analysis.

616 **Protein extraction, immunoprecipitation, and western blot analysis**

617 100 mg soil-grown *A. thaliana* plant leaves or *N. benthamiana* leaves were collected and
618 extracted by extraction buffer (100 mM Tris-HCl pH 8.0, 0.2% SDS and 2% β-

mercaptoethanol). Loading buffer was added to each protein sample and boiled for 5 min. Protein abundance was quantified using ImageJ (https://imagej.nih.gov/ij/).

Co-immunoprecipitation assay was performed as previously described (Wu et al., 2017b). In brief, *N. benthamiana* plants were infiltrated with agrobacteria. About 2.5 g *N. benthamiana* leaves expressing the indicated proteins were harvested at 54 hpi and ground into powder with liquid nitrogen. Extraction buffer contains 25 mM Tris-HCl pH 7.5, 150 mM NaCl, 1mM EDTA, 0.15% Nonidet P-40, 10% Glycerol, 1 mM PMSF, 1× Protease Inhibitor Cocktail (Roche; Cat. #11873580001), and 10 mM DTT. The FLAG-tagged NRG1C and SAG101 proteins were immunoprecipitated using 20 µl M2 beads (Sigma; Cat. #A2220) for co-immunoprecipitation and biotinylation was detected by Streptavidin-HRP (Abcam Cat. # ab7403)

The anti-HA antibody was from Roche (Cat. #11867423001). The anti-FLAG antibody was from Sigma (Cat. #F1804). The anti-EDS1 antibody was generously shared from Dr. Jane E. Parker (Feys et al., 2001).

Statistical analysis

One-way ANOVA followed by Tukey's post hoc test was performed. The Scheffé multiple comparison was applied for testing correction. Normality test for all data was done in SPSS. Statistical significance was indicated with different letters. *p* values and sample numbers (n) were detailed in figure legends.

Acknowledgments

Drs. Jeff Dangl, Jane Parker, Brian Staskawicz, Pingtao Ding, Jonathan Jones, Yu Ti Cheng and Shenyang He are cordially thanked for generous sharing of *A. thaliana* seeds of mutants, anti-EDS1 antibody and *Pseudomonas Avr* strains. Dr. Marc T. Nishimura is thanked for sharing the RBA1 constructs. Dr. Brian J. Staskawicz is thanked for sharing the *nrg1-1 N. benthamiana* seeds. Mr. Kevin Ao and Dr. Paul Kapos are sincerely thanked for careful reading of the manuscript. This work was financially supported by CFI-JELF, the Natural Sciences and Engineering Research Council of Canada (NSERC) Discovery Program, NSERC-CREATE PRoTECT program, and the WD Cooper Memorial Fund from UBC.

Author contributions

ZW, Data curation, Validation, Investigation, Methodology, Writing - original draft, Project administration; LT, Validation, Methodology; X Li, Conceptualization, Data curation, Formal analysis, Supervision, Funding acquisition, Writing—original draft, Project administration, Writing - revisions. All authors reviewed the manuscript.

Conflict of interest

Nothing declared.

Figure legends

Figure 1. *NRG1C* is evolutionarily conserved in Brassicaceae, and its transcription is induced in TNL type autoimmune mutants and upon pathogen infection.

(A) Protein domain diagram of NRG1A, NRG1B and NRG1C. Numbers represent amino acid positions relative to the translation start sites. NRG1C lacks the RPW8 CC and part of the NB domains.

(B) Phylogenetic tree of putative NRG1A/1B/1C orthologs. Putative NRG1A/1B/1C orthologs were obtained from Phytozome (Brassicaceae species) and Sol Genomics Network (*N. benthamiana*) using *A. thaliana* NRG1A, NRG1B and NRG1C protein sequences as input, respectively. ZAR1 was used as an outgroup to root the tree. MUSCLE was used for sequence alignment and a Neighbor-joining tree was generated by using full-length NRG1C and homologous parts of all other corresponding NRG1 homologs with JTT model and using 2000 bootstrap replicates in MEGA 7.0.

(C-D) *NRG1C* (C) and *DAR5* (D) gene expression in the autoimmune mutants *snc1* and *chs3-2D* as determined by RT-PCR (Col-0 serves as wild type control and the transcript level in Col-0 was arbitrarily set at 1.0). Statistical significance is indicated by different letters ($p < 0.01$). Error bars represent means ± SE (Stand Error) (n = 3). Three independent experiments were carried out with similar results.

(E) RT-PCR analysis of the expression of *NRG1C* and *DAR5* after *P.s.m.* ES4326 infection. Samples were collected at 0, 12 and 24 h after infection. Values were

normalized to the level of *ACTIN7* and the transcript levels at 0 h post-inoculation (hpi) were set at 1.0. Error bars represent means ± SE (n = 3). Three independent experiments were carried out with similar results.

Figure 2. *NRG1C* negatively regulates *chs3-2D* and *snc1*-mediated autoimmunity.

(A) Morphology of four-week-old soil-grown plants of Col-0, *chs3-2D*, two independent transgenic lines of *NRG1C OE* into *chs3-2D* background and *chs3-2D nrg1a nrg1b*. *OE* stands for overexpression of *NRG1C*. Bar = 1cm.

(B) *NRG1C* gene expression in the indicated genotypes as determined by RT-PCR (*chs3-2D* serves as control whose *NRG1C* transcript level was set at 1.0). Statistical significance is indicated by different letters ($p < 0.01$). Error bars represent means ± SE (n = 3). Two independent experiments were carried out with similar results.

(C) Fresh weights of plants in (A). Statistical significance is indicated by different letters ($p < 0.01$). Error bars represent means ± SE (n=7).

(D) Quantification of *H.a.* Noco2 sporulation in the indicated genotypes 7 days post inoculation (dpi) with 10^5 spores per ml water. Statistical significance is indicated by different letters ($p < 0.01$). Error bars represent means ± SE (n=4). Three independent experiments were carried out with similar results.

(E) *NRG1C* gene expression in the indicated plants as determined by RT-PCR (*snc1* serves as control whose *NRG1C* transcript level was set at 1.0). Statistical significance is indicated by different letters ($p < 0.01$). Error bars represent means ± SE (n = 3). Two independent experiments were carried out with similar results.

(F) Morphology of four-week-old soil-grown plants of Col-0, *snc1*, two independent transgenic lines of *NRG1C OE* into *snc1* background and *snc1 nrg triple*. Bar = 1cm.

(G) Fresh weights of plants in (F). Statistical significance is indicated by different letters ($p < 0.01$). Error bars represent means ± SE (n=7). The color legends are included in I.

(H) Quantification of *H.a.* Noco2 sporulation in the indicated genotypes at 7 dpi with 10^5 spores per ml water. Statistical significance is indicated by different letters ($p < 0.01$). Error bars represent means ± SE (n=4). Three independent experiments were carried out with similar results. The color legends are included in I.

(I) Bacterial growth of *P.s.t.* DC3000 in four-week-old leaves of the indicated genotypes at 0 and 3 dpi with bacterial inoculum of OD_{600} = 0.001. Statistical significance is indicated by different letters ($p < 0.01$). Error bars represent means ± SE (n=4). Three independent experiments were carried out with similar results.

Figure 3. NRG1C antagonizes HopQ1-1-mediated defense and AvrRPS4-mediated HR.

(A) Growth of *P.s.t.* CUCPB5500 and *P.s.t.* CUCPB5500 HopQ1-1 in four-week-old leaves of the indicated genotypes at 0 and 3 dpi with bacterial inoculum of OD_{600} = 0.0005. Statistical significance is indicated by different letters ($p < 0.01$). Error bars represent means ± SE (n=4). Three independent experiments were carried out with similar results.

(B) HR observation of leaves infiltrated with *Pf0-1*_AvrRPS4. Four-week-old *A. thaliana* leaves of the indicated genotypes were infiltrated with *Pf0-1* expressing AvrRPS4 at OD_{600} = 0.2. Photographs were taken at 36 hpi. The numbers indicate the number of plants displaying HR out of the total number of plants tested. Three independent experiments were carried out with similar results.

(C) Ion leakage of *A. thaliana* leaves upon *Pf0-1*_AvrRPS4 infiltration under the same conditions as for B. Each dot represents four technical replicates from one independent experiment. Statistical significance is indicated by different letters ($p < 0.01$). Error bars represent means ± SE (n=3). Three independent experiments were carried out with similar results.

Figure 4. NRG1C works along the EDS1-NRG1-SAG101 module, in parallel with the EDS1-ADR1-PAD4 module.

(A) Morphology of four-week-old soil-grown plants of Col-0, *snc1*, *snc1 eds1-2*, *snc1 pad4-1*, *snc1 adr1 triple*, *snc1 sag101-1*, *snc1 nrg triple*, *snc1 pad4-c1 adr1 triple*, *snc1 sag101-1 nrg triple*, *snc1 pad4-c1 sag101-1*, *snc1 pad4-c1 nrg triple*, *snc1 sag101-c1 adr1 triple* and *snc1 adr1 triple nrg triple*. *pad4-c1* and *sag101-c1* alleles were generated through the CRISPR-Cas9 system. Bar = 1cm.

(B) *PR1* gene expression in the indicated genotypes as determined by RT-PCR (Col-0 serves as control whose *PR1* transcript level was set at 1.0). Statistical significance is indicated by different letters ($p < 0.01$). Error bars represent means ± SE (n = 3). Two independent experiments were carried out with similar results.

(C) Morphology of four-week-old soil-grown plants of Col-0, *snc1*, *snc1 nrg triple*, *snc1 sag101-1*, *snc1 NRG1C* OE, *snc1 nrg triple NRG1C OE* and *snc1 sag101-1 NRG1C OE*. *OE* stands for overexpression of *NRG1C*. Bar = 1cm.

Figure 5. NRG1C regulates *chs3-2D*-mediated autoimmunity through processes unrelated to transcriptional interference.

(A) Morphology of four-week-old soil-grown plants of Col-0, *chs3-2D*, and two independent transgenic lines of $NRG1C^{T71*}$ *OE* into *chs3-2D* background. *OE* stands for overexpression of $NRG1C^{T71*}$, which carries an early stop codon to disrupt protein synthesis, but not transcription. Bar = 1cm.

(B) $NRG1C^{T71*}$ gene expression in the indicated genotypes as determined by RT-PCR (*chs3-2D* serves as control whose *NRG1C* transcript level was set at 1.0). Statistical significance is indicated by different letters ($p < 0.01$). Error bars represent means ± SE (n = 3). Two independent experiments were carried out with similar results.

(C) Fresh weights of plants in (A). Statistical significance is indicated by different letters ($p < 0.01$). Error bars represent means ± SE (n=7).

(D) Quantification of *H.a.* Noco2 sporulation in the indicated genotypes at 7 dpi with 10^5 spores per ml water. Statistical significance is indicated by different letters ($p < 0.01$). Error bars represent means ± SE (n=4). Three independent experiments were carried out with similar results.

Figure 6. NRG1C associates with EDS1-SAG101 complex.

(A) Immunoprecipitation and biotinylation of NRG1C-3FLAG and SAG101-3FLAG by EDS1-HA-TurboID in *N. benthamiana* in the presence of RBA1. Immunoprecipitation was carried out with anti-FLAG beads. The 3FLAG-tagged proteins were detected using an anti-FLAG antibody. The HA-TurboID-tagged proteins were detected using an anti-HA antibody. The biotinylated proteins were detected using Streptavidin-HRP. Molecular

mass marker in kiloDaltons is indicated on the left. The experiment was repeated three times with similar results.

(B) Biotinylation of SAG101-3FLAG by NRG1C-HA-TurboID in *A. thaliana* plants stably transformed with the two transgenes in the presence of RBA1. Immunoprecipitation was carried out with anti-FLAG beads. The 3FLAG-tagged proteins were detected using an anti-FLAG antibody. The HA-TurboID-tagged proteins were detected using an anti-HA antibody. EDS1 was detected using an anti-EDS1 antibody. The biotinylated proteins were detected using HRP-Streptavidin. Molecular mass marker in kiloDaltons is indicated on the left. The experiment was repeated twice with similar results.

Figure 7. NRG1C-type N-terminally truncated hNLRs from canola (*Brassica napus* L. cv. Westar) and *N. benthamiana* function similarly as *A. thaliana* NRG1C.

(A) Morphology of four-week-old soil-grown plants of Col-0, *chs3-2D*, and two independent transgenic lines of *BraNRG1C OE* into *chs3-2D* background. Bar = 1cm.

(B) *BraNRG1C* gene expression in the indicated plants as determined by RT-PCR. Statistical significance is indicated by different letters ($p < 0.01$). Error bars represent means ± SE (n = 3). ND stands for Not Detectable. Two independent experiments were carried out with similar results. The color legends are included in D.

(C) Fresh weights of plants in (A). Statistical significance is indicated by different letters ($p < 0.01$). Error bars represent means ± SE (n=7). The color legends are included in D.

(D) Quantification of *H.a.* Noco2 sporulation in the indicated genotypes at 7 dpi with 10^5 spores per ml water. Statistical significance is indicated by different letters ($p < 0.01$). Error bars represent means ± SE (n=4). Three independent experiments were carried out with similar results.

(E-F) HR observation of *N. benthamiana* leaves expressing the indicated proteins at 48 hpi following the infiltration of *P.s.t.* CUCPB5500 HopQ1-1 to deliver HopQ1-1 effector. Photographs were taken at 4 dpi after *P.s.t.* CUCPB5500 HopQ1-1 infiltration.

(G-H) Ion leakage of *N. benthamiana* leaves upon *P.s.t.* CUCPB5500 HopQ1-1 infiltration under the same conditions as with E and F. Statistical significance is indicated

by different letters ($p < 0.01$). Error bars represent means ± SE (n = 6). Three independent experiments were carried out with similar results.

(I) A model of two defense modules downstream of NRG1-dependent-TNL activation in Arabidopsis. An effector-induced TNL resistosome with NADase activity (Horsefield et al., 2019; Ma et al., 2020; Martin et al., 2020; Tian and Li, 2020; Wan et al., 2019) signals through two parallel modules, EDS1-PAD4-ADR1s and EDS1-SAG101-NRG1A/1B to activate defense responses. N-terminally truncated hNLR NRG1C antagonizes immunity mediated by its full-length neighbors NRG1A and NRG1B to avoid aberrant activation.

Supplemental Figure 1. Full-length protein sequence alignment of NRG1C and its orthologs in different plant species. (Supports Figure 1A-B)

Putative NRG1C orthologs were obtained from Phytozome (Brassicaceae species) and Sol Genomics Network (*N. benthamiana*) using *A. thaliana* NRG1C protein sequence as input. NB domain and LRR domain are indicated by single underline and double underline, respectively. P-loop motif is boxed in a black line.

Supplemental Figure 2. DAR5 has no effect on *chs3-2D* and *snc1*-mediated autoimmunity. (Supports Figure 1D-E)

(A) Morphology of four-week-old soil-grown plants of Col-0, *chs3-2D*, and two independent transgenic lines of *DAR5 OE* into *chs3-2D* background. *OE* stands for overexpression of *DAR5*. Bar = 1cm.

(B) *DAR5* gene expression in the indicated plants as determined by RT-PCR (*chs3-2D* serves as control whose *DAR5* transcript level was set at 1.0). Statistical significance is indicated by different letters ($p < 0.01$). Error bars represent means ± SE (n = 3). Two independent experiments were carried out with similar results.

(C) Morphology of four-week-old soil-grown plants of Col-0, *snc1*, and two independent transgenic lines of *DAR5 OE* into *snc1* background. *OE* stands for overexpression of *DAR5*. Bar = 1cm.

(D) *DAR5* gene expression in the indicated plants as determined by RT-PCR (*snc1* serves as control whose *DAR5* transcript level was set at 1.0). Statistical significance is indicated

by different letters ($p < 0.01$). Error bars represent means ± SE (n = 3). Two independent experiments were carried out with similar results.

Supplemental Figure 3. Full-length protein sequence alignment of ADR1-L3 and its orthologs in different plant species. (Supports Figure 1)

Putative ADR1-L3 orthologs were obtained from Phytozome using *A. thaliana* ADR1-L3 protein sequence as input. RPW8 domain, NB domain and LRR domain are indicated by single underline, double underline and dashed underline, respectively.

Supplemental Figure 4. No immune-related phenotypes were observed in *ADR1-L3* overexpression lines. (Supports Figure 1 and Supplemental Figure 3)

(A) Morphology of four-week-old soil-grown plants of Col-0, *snc1*, and two independent transgenic lines of *ADR1-L3 OE* into *snc1* background. *OE* stands for overexpression of *ADR1-L3*. Bar = 1cm.

(B) Quantification of *H.a.* Noco2 sporulation in the indicated genotypes at 7 dpi with 10^5 spores per ml water. Statistical significance is indicated by different letters ($p < 0.01$). Error bars represent means ± SE (n=4). Three independent experiments were carried out with similar results.

(C) Quantification of *H.a.* Emwa1 sporulation in the indicated genotypes at 7 dpi with 10^5 spores per ml water. Statistical significance is indicated by different letters ($p < 0.01$). Error bars represent means ± SE (n=4). Three independent experiments were carried out with similar results.

Supplemental Figure 5. Overexpression of *NRG1C* has no effect on *chs1-2* or *chs2-1*-mediated autoimmunity. (Supports Figure 2)

(A-B) Morphology of four-week-old soil-grown plants of Col-0, *chs1-2* (A), *chs2-1* (B) and two independent transgenic lines of *NRG1C OE* into *chs1-2* (A) and *chs2-1* (B) backgrounds. Plants were grown at 16 °C under long day conditions. Bar = 1cm.

(C) Morphology of four-week-old soil-grown plants of Col-0 and two independent transgenic lines of *NRG1C OE* in Col-0 background. Bar = 1cm.

(D) Quantification of *H.a.* Emwa1 sporulation in the indicated genotypes at 7 dpi with 10^5 spores per ml water. Statistical significance is indicated by different letters ($p < 0.01$). Error bars represent means ± SE (n=4). Three independent experiments were carried out with similar results.

Supplemental Figure 6. NRG1C does not affect TNL RPS4 or CNL RPS2-mediated bacterial growth and basal defense. (Supports Figure 2-3)

(A-C) Growth of *P.s.t. avrRps4* (A), *avrRpt2* (B) and *P.s.t.* DC3000 (C) in four-week-old leaves of the indicated genotypes at 0 dpi and 3 dpi with bacterial inoculum of OD_{600} = 0.001. Statistical significance is indicated by different letters ($p < 0.01$). Error bars represent means ± SE (n=4). Three independent experiments were carried out with similar results.

Supplemental Figure 7. Schematic description of CRISPR/Cas9 construct design to delete *PAD4* or *SAG101*. (Supports Figure 4A)

Red arrows indicate the location of two guide RNA target sites. Target sequences are shown in the below. The letters in red indicate the NGG PAM sequences. Scissors indicate where the Cas9 cut the genomic sequence.

Supplemental Figure 8. NRG1C works in the same pathway with the EDS1-NRG1-SAG101 module. (Supports Figure 4C)

(A-B) *PR1* gene expression in the indicated genotypes as determined by RT-PCR (Col-0 serves as control whose *PR1* transcript level was set at 1.0). Statistical significance is indicated by different letters ($p < 0.01$). Error bars represent means ± SE (n = 3). Two independent experiments were carried out with similar results.

Supplemental Figure 9. NRG1C antagonizes NRG1A D485V-mediated HR. (Supports Figure 6)

(A) HR in the *N. benthamiana* leaves expressing NRG1A D485V-3FLAG and EV (Empty Vector) in the absence (right) or presence (left) of NRG1C. Photos were taken at 4 dpi. Three independent experiments were carried out with similar results.

(B) Ion leakage of *N. benthamiana* leaves upon *Agrobacterium* infiltration under the same conditions as for B. Statistical significance is indicated by different letters ($p < 0.01$). Error bars represent means ± SE (n = 3). Three independent experiments were carried out with similar results.

(C) Immunoblot analysis of protein levels of NRG1A D485V-3FLAG in leaves of B. Samples were harvest at 24 hpi, when no macroscopic HR was visible. Equal loading is shown by Ponceau S staining of a non-specific band. The numbers below represent the normalized ratio between the intensity of the protein band and the Ponceau S band ± SE (n=3). Molecular mass marker in kiloDaltons is indicated on the left.

Supplemental Figure 10. NRG1C does not influence the autoimmunity of *ADR1-L2 D484V*. (Supports Figure 6)

(A) Morphology of three-week-old soil-grown plants of Col-0, *ADR1-L2 D484V*, and two independent transgenic lines of *NRG1C OE* into *ADR1-L2 D484V* background. *OE* stands for overexpression of *NRG1C*. Bar = 1cm.

(B) Fresh weights of plants in (A). Statistical significance is indicated by different letters ($p < 0.01$). Error bars represent means ± SE (n=7).

(C) Quantification of *H.a.* Noco2 sporulation in the indicated genotypes at 7 dpi with 10^5 spores per ml water. Statistical significance is indicated by different letters ($p < 0.01$). Error bars represent means ± SE (n=4). Three independent experiments were carried out with similar results.

Supplemental Figure 11. NRG1C does not associate with full-length NRG1A. (Supports Figure 6)

(A) HR in the WT or *nrg1-1 N. benthamiana* leaves expressing RBA1. Photos were taken at 2 dpi. Three independent experiments were carried out with similar results.

(B) Immunoprecipitation of NRG1C-3FLAG and biotinylation of NRG1C-3FLAG by NRG1A-HATurboID in *N. benthamiana* in the presence of RBA1. Immunoprecipitation was carried out with anti-FLAG beads. The 3FLAG-tagged proteins were detected using an anti-FLAG antibody. The HA-TurboID-tagged proteins were detected using an anti-HA antibody. The biotinylated proteins were detected using Streptavidin-HRP. Molecular

mass marker in kiloDaltons is indicated on the left. Three independent experiments were carried out with similar results.

Supplemental Figure 12. The association between NRG1C with EDS1-SAG101 complex depends on TIR induction and SAG101. (Supports Figure 6)

(A) Immunoprecipitation and biotinylation of NRG1C-3FLAG and SAG101-3FLAG by EDS1-HA-TurboID in *N. benthamiana* in the absence of RBA1. Immunoprecipitation was carried out with anti-FLAG beads. The 3FLAG-tagged proteins were detected using an anti-FLAG antibody. The HA-TurboID-tagged proteins were detected using an anti-HA antibody. The biotinylated proteins were detected using Streptavidin-HRP. Molecular mass marker in kiloDaltons is indicated on the left. Three independent experiments were carried out with similar results.

(B) Immunoprecipitation and biotinylation of NRG1C-3FLAG or/and SAG101-3FLAG by EDS1-HA-TurboID in *N. benthamiana*. Immunoprecipitation was carried out with anti-FLAG beads. The 3FLAG-tagged proteins were detected using an anti-FLAG antibody. The HA-TurboID-tagged proteins were detected using an anti-HA antibody. The biotinylated proteins were detected using Streptavidin-HRP. Molecular mass marker in kiloDaltons is indicated on the left. Three independent experiments were carried out with similar results.

Supplemental Figure 13. Overexpression of *NRG1C* does not affect the protein levels of EDS1 and SAG101. (Supports Figure 6)

(A) Immunoblot analysis of protein levels of EDS1-ZZ-TEV-FLAG in the absence or presence of NRG1C-3FLAG. Equal loading is shown by Ponceau S staining of a non-specific band. Molecular mass marker in kiloDaltons is indicated on the left.

(B) Quantification of band intensity of (A). The numbers represent the normalized ratio between the intensity of the protein band and the Ponceau S band ± SE (n=8).

(C) Immunoblot analysis of protein levels of SAG101-3FLAG in the absence or presence of NRG1C-3FLAG. Equal loading is shown by Ponceau S staining of a non-specific band. Molecular mass marker in kiloDaltons is indicated on the left.

(D) Quantification of band intensity of C. The numbers represent the normalized ratio between the intensity of the protein band and the Ponceau S band ± SE (n=8).

Supplemental Figure 14. TIR NADase enzyme activity promotes the association between NRG1C with EDS1-SAG101 complex, and NRG1C does not associate with the EDS1-PAD4 complex. (Supports Figure 6)

(A) Immunoprecipitation and biotinylation of NRG1C-3FLAG and SAG101-3FLAG by EDS1-HA-TurboID in *N. benthamiana* in the presence of $RBA1_{E86A}$. Immunoprecipitation was carried out with anti-FLAG beads. The 3FLAG-tagged proteins were detected using an anti-FLAG antibody. The HA-TurboID-tagged proteins were detected using an anti-HA antibody. The biotinylated proteins were detected using Streptavidin-HRP. Molecular mass marker in kiloDaltons is indicated on the left. Three independent experiments were carried out with similar results.

(B) Immunoprecipitation and biotinylation of NRG1C-3FLAG and PAD4-ZZ-TEV-FLAG by EDS1-HA-TurboID in *N. benthamiana* in the presence of RBA1. Immunoprecipitation was carried out with anti-FLAG beads. The ZZ-TEV-FLAG and 3FLAG-tagged proteins were detected using an anti-FLAG antibody. The HA-TurboID-tagged proteins were detected using an anti-HA antibody. The biotinylated proteins were detected using Streptavidin-HRP. Molecular mass marker in kiloDaltons is indicated on the left. Three independent experiments were carried out with similar results.

(C) The normalized ratio between the intensity of the NRG1C band and the SAG101 band in different treatments. As EDS1 constitutively associates with SAG101, SAG101 bands were used as controls.

Supplemental Figure 15. Brassicaceae NRG1C ortholog does not influence HopQ1-1-mediated HR in *N. benthamiana*. (Supports Figure 7)

(A) Schematic showing *N. benthamiana* transient expression assays to test protein functionalities in HopQ1-1-dependent HR by infiltrating with *P.s.t.* CUCPB5500 HopQ1-1 (see Methods for details).

(B-C) *NbNRG2* (B) and *NRG1C* (C) genes expression in the indicated leaves as determined by RT-PCR. Statistical significance is indicated by different letters ($p < 0.01$).

Error bars represent means ± SE (n = 3). The *NbNRG2* transcript level in the presence of EV treatment was set at 1.0. Two independent experiments were carried out with similar results.

(D) HR in the *N. benthamiana* leaves expressing the indicated proteins at 48 hpi following the infiltration of *P.s.t.* CUCPB5500 HopQ1-1 to deliver HopQ1-1 effector. Photographs were taken at 4 dpi after *P.s.t.* CUCPB5500 HopQ1-1 infiltration.

(E) Ion leakage of *N. benthamiana* leaves upon *P.s.t.* CUCPB5500 HopQ1-1 infiltration in the same conditions as for the photographs in D. Statistical significance is indicated by different letters ($p < 0.01$). Error bars represent means ± SE (n = 6). Three independent experiments were carried out with similar results.

(F) *BraNRG1C* gene expression in the indicated leaves as determined by RT-PCR. Error bars represent means ± SE (n = 3). Two independent experiments were carried out with similar results.

Supplemental Figure 16. NbNRG2 does not influence *chs3-2D*-mediated autoimmunity. (Supports Figure 7)

(A) Morphology of four-week-old soil-grown plants of Col-0, *chs3-2D*, and two independent transgenic lines of *NbNRG2 OE* into *chs3-2D* background. *OE* stands for overexpression of *NbNRG2*. Bar = 1cm.

(B) *NbNRG2* expression level in the indicated plants as determined by RT-PCR. Statistical significance is indicated by different letters ($p < 0.05$). Error bars represent means ± SE (n = 3). Three independent experiments were carried out with similar results.

(C) Fresh weights of plants in (A). Statistical significance is indicated by different letters ($p < 0.01$). Error bars represent means ± SE (n=6).

(D) Quantification of *H.a.* Noco2 sporulation in the indicated genotypes at 7 dpi with 10^5 spores per ml water. Statistical significance is indicated by different letters ($p < 0.01$). Error bars represent means ± SE (n=4). Three independent experiments were carried out with similar results.

Supplemental Table 1. The genome arrangement of NRG1C in plant species.

Arrows in tandem indicate tandemly arranged genes, while arrows in rows indicate randomly assorted genes on different scaffolds. All sequences were obtained from Phytozome. *A. thaliana* (*AT5G66910*, *AT5G66900*, *AT5G66890*); *Arabidopsis lyrate* (*AL8G44490*, *AL8G44500*, *AL8G44510*); *Arabidopsis haller* (*Araha.11408s0003.1*, *Araha.11408s0002.1*); *Boechera stricta* (*Bostr.27102s0001.1*; *Bostr.0568s0113.1*); *Capsella grandiflora* (*Cagra.2007s0011.1*, *Cagra.2007s0012.1*); *Capsella rubella* (*Carubv 10027991m*, *Carubv10028036m*); *Eutrema salsugineum* (*Thhalv10003662m*, *Thhalv10005443m*, *Thhalv10005517m*; *Thhalv10020099m*); *Brassica rapa* (*Brara.I00877.1*, *Brara.I00876.1*; *Brara.G01212.1*, *Brara.G01211.1*; *Brara.B03562.1*; *Brara.F02778.1*). All truncated NRG1C orthologs are labeled with yellow arrows. Orange arrow indicates *Brara*.G01211.1.

Supplemental Table 2. The genome arrangement of *NL* truncated genes in *A. thaliana*.

Arrows in tandem indicate tandemly arranged genes. Dashed line indicates two genes are clustered, but not tandemly arranged. Gene codes are shown under the arrows. Orange, yellow, black, and blue arrows indicate CN, NL, full-length NLR, TIR-only proteins, respectively.

Supplemental Table 3. The list of primers used in this study.

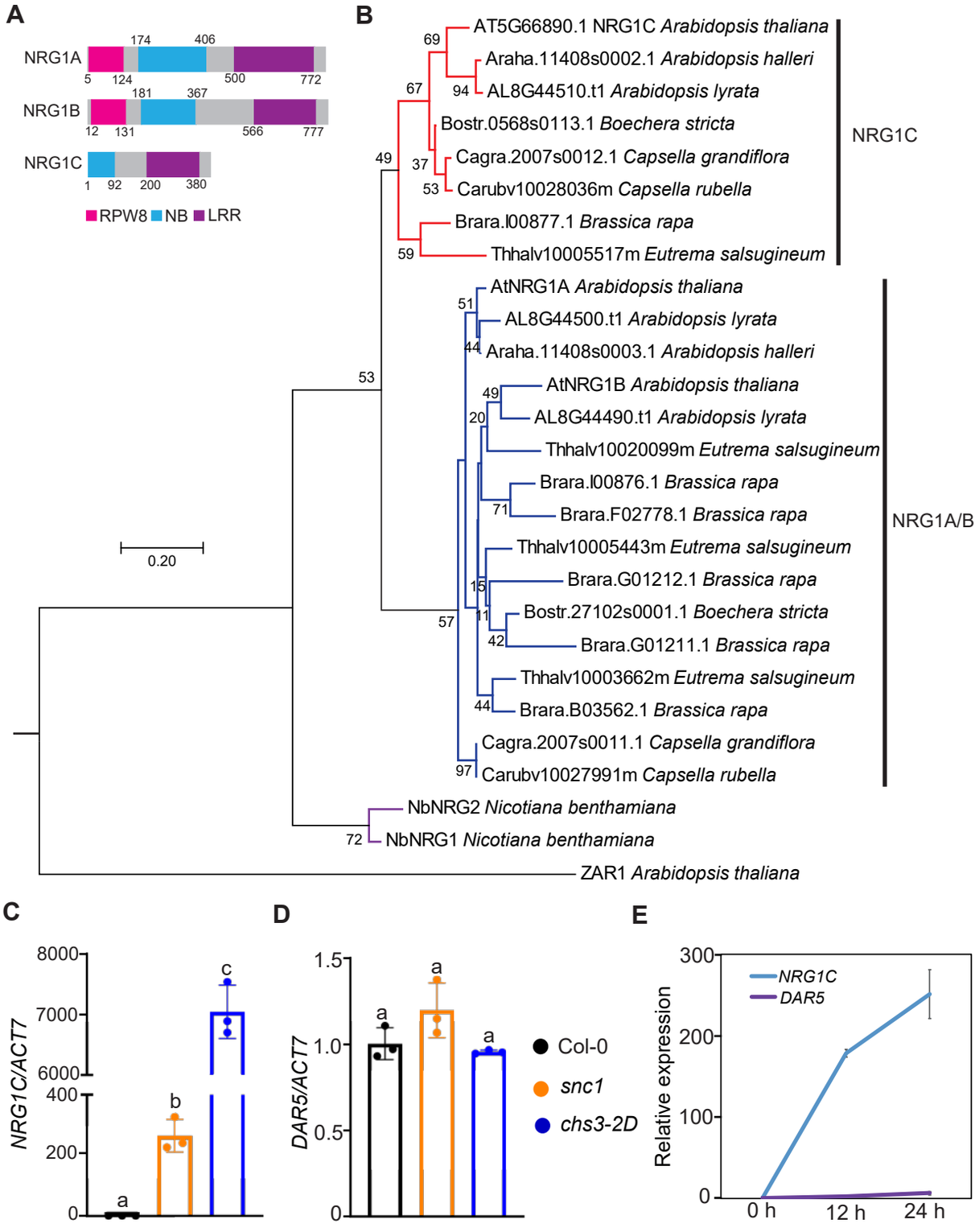

Figure 1. *NRG1C* is evolutionarily conserved in Brassicaceae, and its transcription is induced in TNL type autoimmune mutants and upon pathogen infection.

(A) Protein domain diagram of NRG1A, NRG1B and NRG1C. Numbers represent amino acid positions relative to the translation start sites. NRG1C lacks the RPW8 CC and part of the NB domains.

(B) Phylogenetic tree of putative NRG1A/1B/1C orthologs. Putative NRG1A/1B/1C orthologs were obtained from Phytozome (Brassicaceae species) and Sol Genomics Network (*N. benthamiana*) using *A. thaliana* NRG1A, NRG1B and NRG1C protein sequences as input, respectively. ZAR1 was used as an outgroup to root the tree. MUSCLE was used for sequence alignment and a Neighbor-joining tree was generated by using full-length NRG1C and homologous parts of all other corresponding NRG1 homologs with JTT model and using 2000 bootstrap replicates in MEGA 7.0.

(C-D) *NRG1C* (C) and *DAR5* (D) gene expression in the autoimmune mutants *snc1* and *chs3-2D* as determined by RT-PCR (Col-0 serves as wild type control and the transcript level in Col-0 was arbitrarily set at 1.0). Statistical significance is indicated by different letters ($p < 0.01$). Error bars represent means ± SE (Stand Error) (n = 3). Three independent experiments were carried out with similar results.

(E) RT-PCR analysis of the expression of *NRG1C* and *DAR5* after *P.s.m.* ES4326 infection. Samples were collected at 0, 12 and 24 h after infection. Values were normalized to the level of *ACTIN7* and the transcript levels at 0 h post-inoculation (hpi) were set at 1.0. Error bars represent means ± SE (n = 3). Three independent experiments were carried out with similar results.

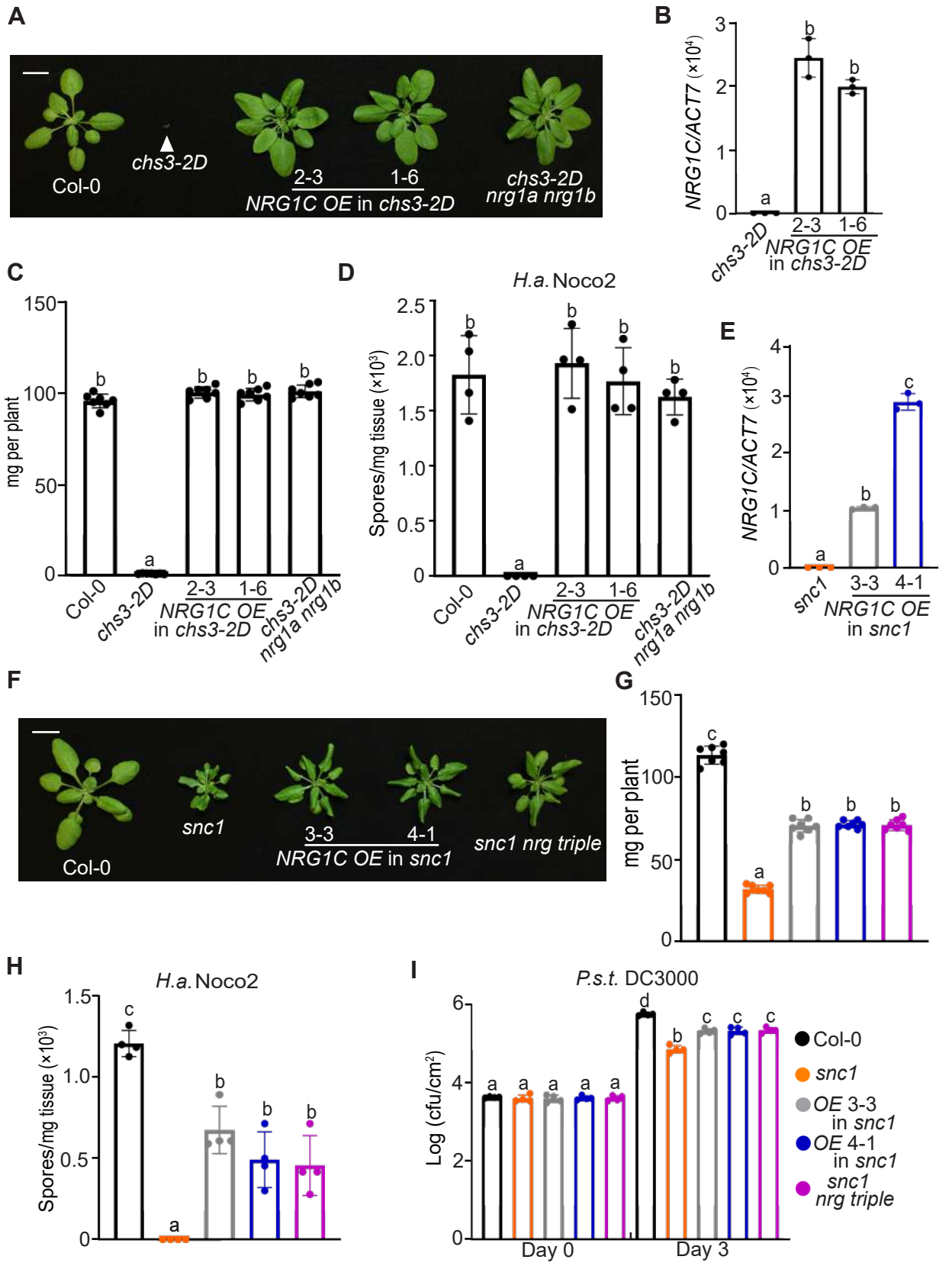

Figure 2. *NRG1C* negatively regulates *chs3-2D* and *snc1*-mediated autoimmunity.
(A) Morphology of four-week-old soil-grown plants of Col-0, *chs3-2D*, two independent transgenic lines of *NRG1C OE* into *chs3-2D* background and *chs3-2D nrg1a nrg1b*. *OE* stands for overexpression of *NRG1C*. Bar = 1cm.
(B) *NRG1C* gene expression in the indicated genotypes as determined by RT-PCR (*chs3-2D* serves as control whose *NRG1C* transcript level was set at 1.0). Statistical significance is indicated by different letters ($p < 0.01$). Error bars represent means ± SE (n = 3). Two independent experiments were carried out with similar results.
(C) Fresh weights of plants in (A). Statistical significance is indicated by different letters ($p < 0.01$). Error bars represent means ± SE (n=7).
(D) Quantification of *H.a.* Noco2 sporulation in the indicated genotypes 7 days post inoculation (dpi) with 10^5 spores per ml water. Statistical significance is indicated by different letters ($p < 0.01$). Error bars represent means ± SE (n=4). Three independent experiments were carried out with similar results.
(E) *NRG1C* gene expression in the indicated plants as determined by RT-PCR (*snc1* serves as control whose *NRG1C* transcript level was set at 1.0). Statistical significance is indicated by different letters ($p < 0.01$). Error bars represent means ± SE (n = 3). Two independent experiments were carried out with similar results.
(F) Morphology of four-week-old soil-grown plants of Col-0, *snc1*, two independent transgenic lines of *NRG1C OE* into *snc1* background and *snc1 nrg triple*. Bar = 1cm.
(G) Fresh weights of plants in (F). Statistical significance is indicated by different letters ($p < 0.01$). Error bars represent means ± SE (n=7). The color legends are included in I.
(H) Quantification of *H.a.* Noco2 sporulation in the indicated genotypes at 7 dpi with 10^5 spores per ml water. Statistical significance is indicated by different letters ($p < 0.01$). Error bars represent means ± SE (n=4). Three independent experiments were carried out with similar results. The color legends are included in I.
(I) Bacterial growth of *P.s.t.* DC3000 in four-week-old leaves of the indicated genotypes at 0 and 3 dpi with bacterial inoculum of $OD_{600} = 0.001$. Statistical significance is indicated by different letters ($p < 0.01$). Error bars represent means ± SE (n=4). Three independent experiments were carried out with similar results.

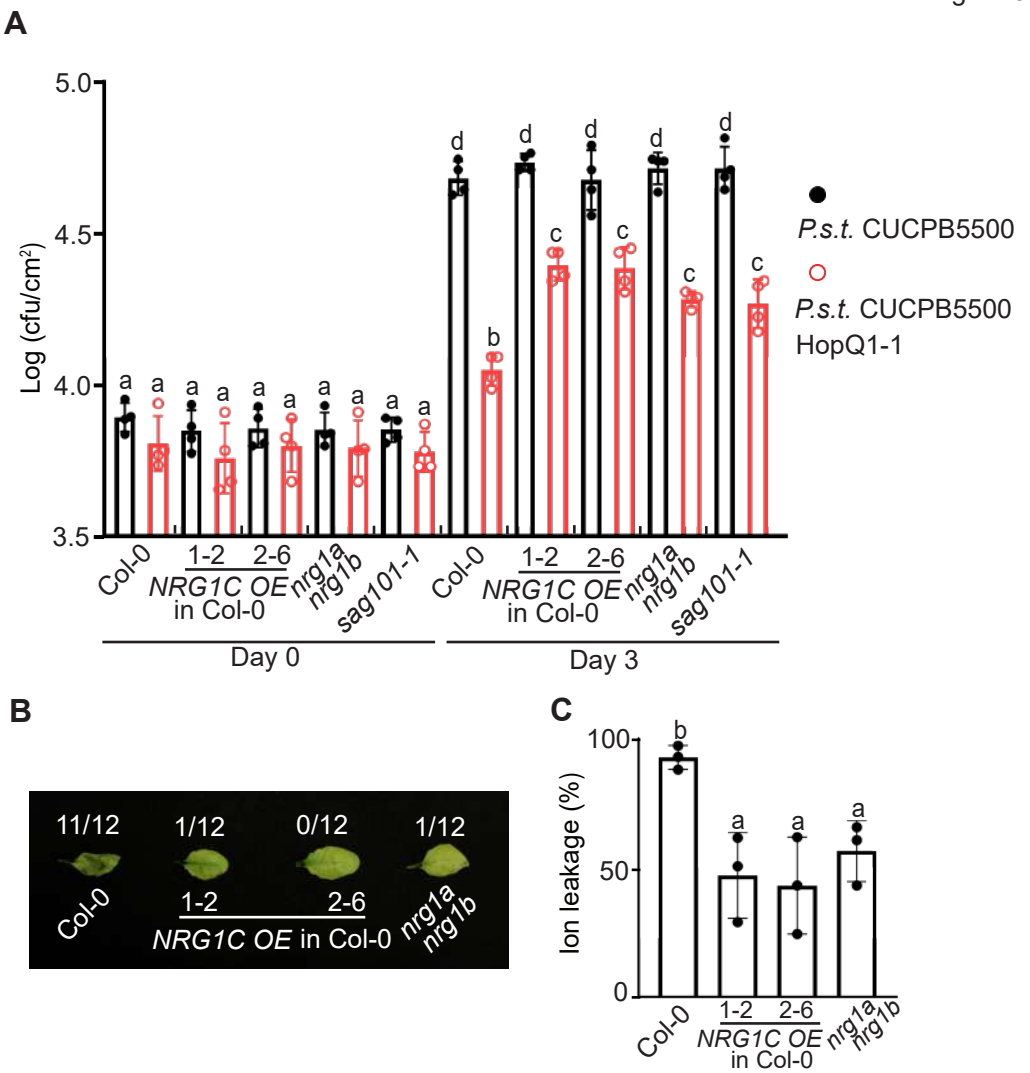

Figure 3. NRG1C antagonizes HopQ1-1-mediated defense and AvrRPS4-mediated HR.

(A) Growth of *P.s.t.* CUCPB5500 and *P.s.t.* CUCPB5500 HopQ1-1 in four-week-old leaves of the indicated genotypes at 0 and 3 dpi with bacterial inoculum of OD_{600} = 0.0005. Statistical significance is indicated by different letters ($p < 0.01$). Error bars represent means ± SE (n=4). Three independent experiments were carried out with similar results.

(B) HR observation of leaves infiltrated with *Pf0-1*_AvrRPS4. Four-week-old *A. thaliana* leaves of the indicated genotypes were infiltrated with *Pf0-1* expressing AvrRPS4 at OD_{600} = 0.2. Photographs were taken at 36 hpi. The numbers indicate the number of plants displaying HR out of the total number of plants tested. Three independent experiments were carried out with similar results.

(C) Ion leakage of *A. thaliana* leaves upon *Pf0-1*_AvrRPS4 infiltration under the same conditions as for B. Each dot represents four technical replicates from one independent experiment. Statistical significance is indicated by different letters ($p < 0.01$). Error bars represent means ± SE (n=3). Three independent experiments were carried out with similar results.

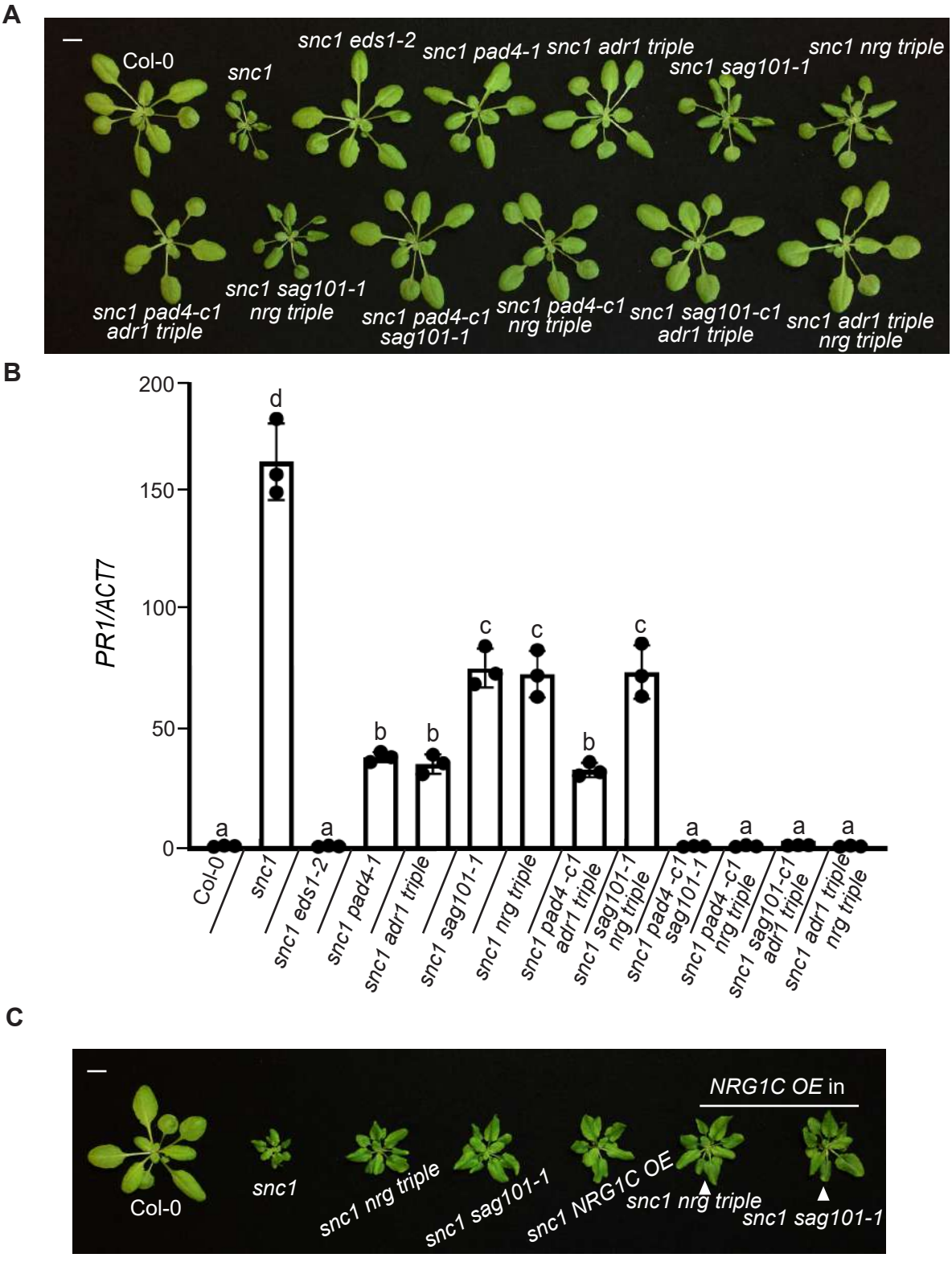

Figure 4. NRG1C works along the EDS1-NRG1-SAG101 module, in parallel with the EDS1-ADR1-PAD4 module.

(A) Morphology of four-week-old soil-grown plants of Col-0, *snc1*, *snc1 eds1*-2, *snc1 pad4-1*, *snc1 adr1 triple*, *snc1 sag101-1*, *snc1 nrg triple*, *snc1 pad4-c1 adr1 triple*, *snc1 sag101-1 nrg triple*, *snc1 pad4-c1 sag101-1*, *snc1 pad4-c1 nrg triple*, *snc1 sag101-c1 adr1 triple* and *snc1 adr1 triple nrg triple*. *pad4-c1* and *sag101-c1* alleles were generated through the CRISPR-Cas9 system. Bar = 1cm.

(B) *PR1* gene expression in the indicated genotypes as determined by RT-PCR (Col-0 serves as control whose *PR1* transcript level was set at 1.0). Statistical significance is indicated by different letters ($p < 0.01$). Error bars represent means ± SE (n = 3). Two independent experiments were carried out with similar results.

(C) Morphology of four-week-old soil-grown plants of Col-0, *snc1*, *snc1 nrg triple*, *snc1 sag101-1*, *snc1 NRG1C* OE, *snc1 nrg triple NRG1C OE* and *snc1 sag101-1 NRG1C OE*. *OE* stands for overexpression of *NRG1C*. Bar = 1cm.

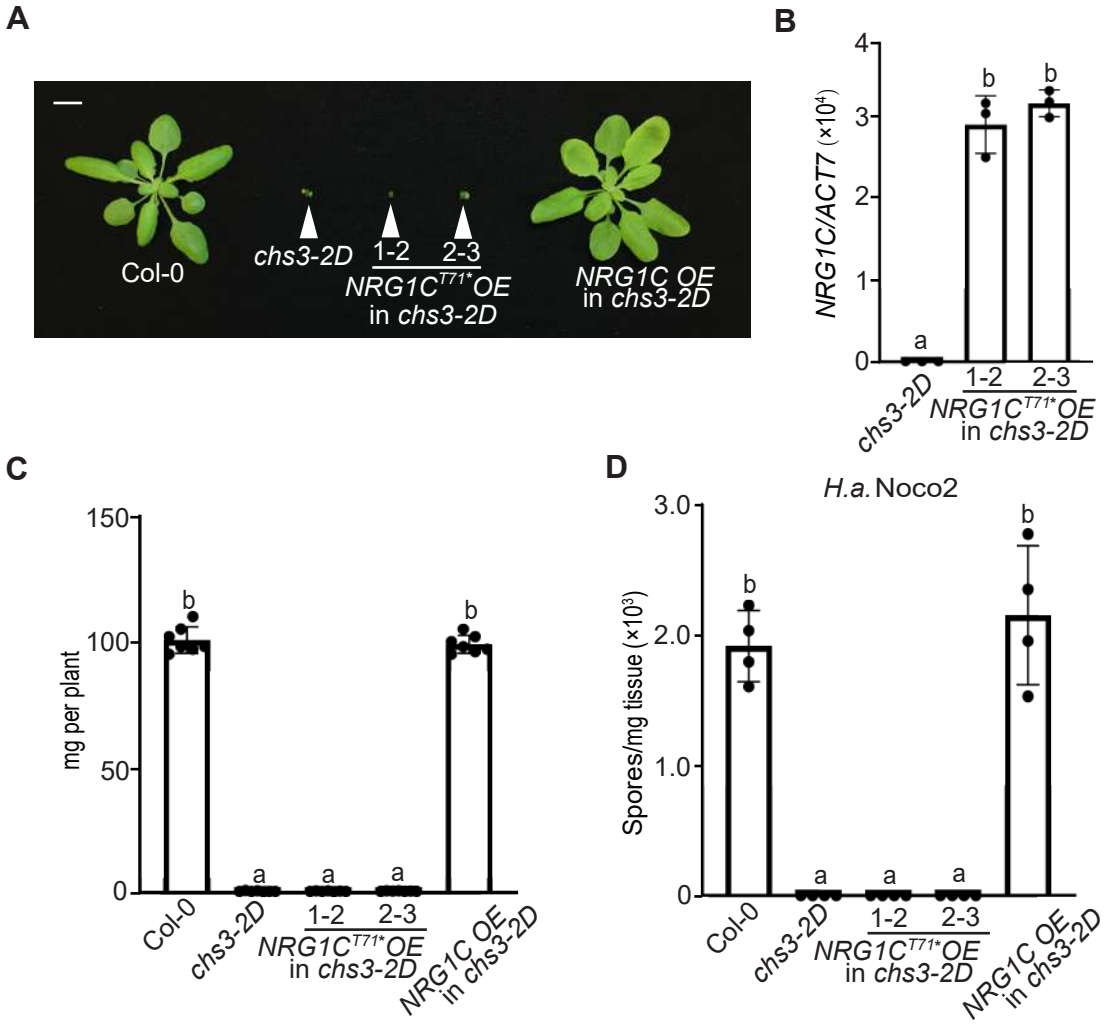

Figure 5. NRG1C regulates *chs3-2D*-mediated autoimmunity through processes unrelated to transcriptional interference.

(A) Morphology of four-week-old soil-grown plants of Col-0, *chs3-2D*, and two independent transgenic lines of *NRG1C*^{T71*} *OE* into *chs3-2D* background. *OE* stands for overexpression of *NRG1C*^{T71*}, which carries an early stop codon to disrupt protein synthesis, but not transcription. Bar = 1cm.

(B) *NRG1C*^{T71*} gene expression in the indicated genotypes as determined by RT-PCR (*chs3-2D* serves as control whose *NRG1C* transcript level was set at 1.0). Statistical significance is indicated by different letters ($p < 0.01$). Error bars represent means ± SE (n = 3). Two independent experiments were carried out with similar results.

(C) Fresh weights of plants in (A). Statistical significance is indicated by different letters ($p < 0.01$). Error bars represent means ± SE (n=7).

(D) Quantification of *H.a.* Noco2 sporulation in the indicated genotypes at 7 dpi with 10^5 spores per ml water. Statistical significance is indicated by different letters ($p < 0.01$). Error bars represent means ± SE (n=4). Three independent experiments were carried out with similar results.

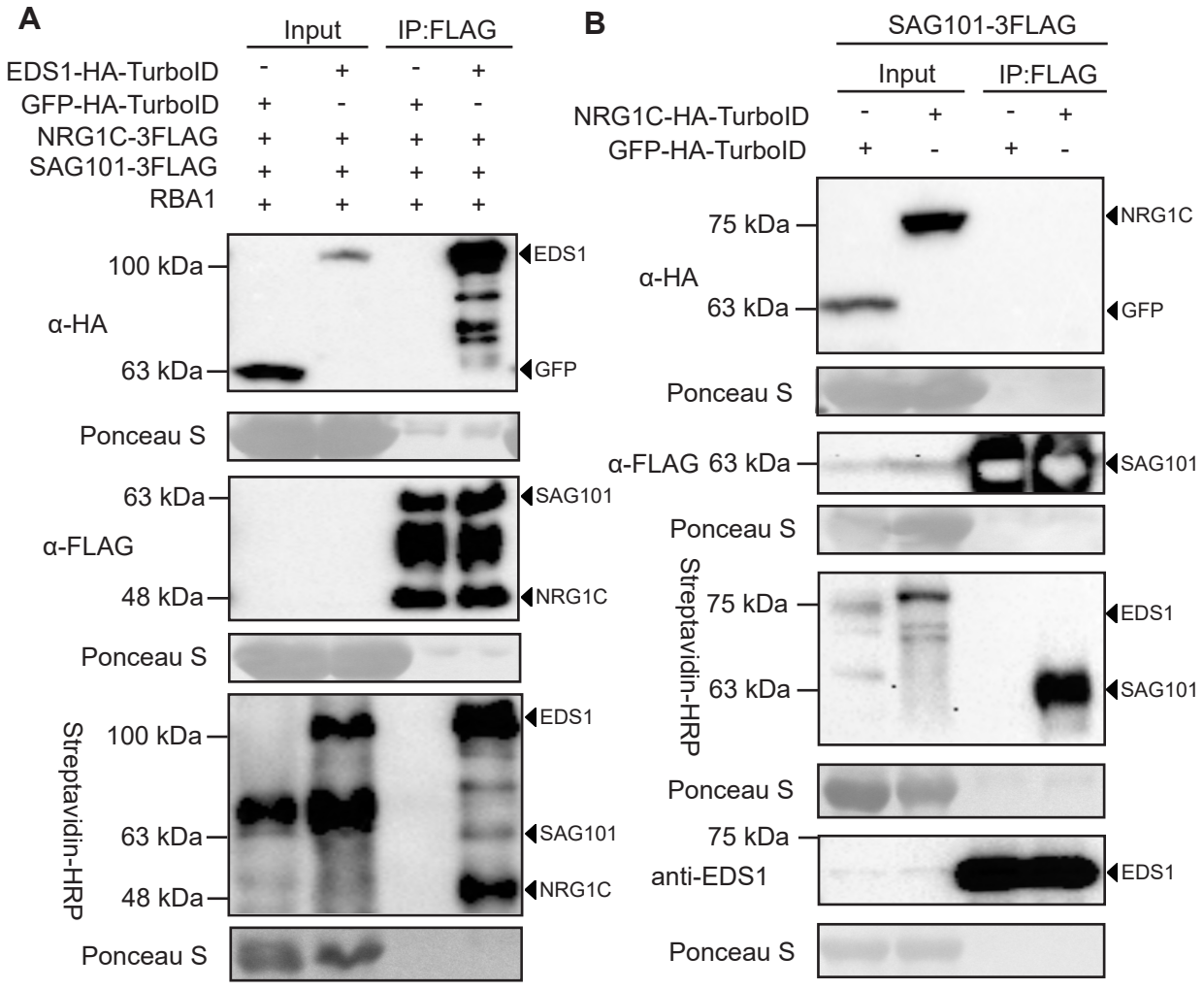

Figure 6. NRG1C associates with EDS1-SAG101 complex.
(A) Immunoprecipitation and biotinylation of NRG1C-3FLAG and SAG101-3FLAG by EDS1-HA-TurboID in *N. benthamiana* in the presence of RBA1. Immunoprecipitation was carried out with anti-FLAG beads. The 3FLAG-tagged proteins were detected using an anti-FLAG antibody. The HA-TurboID-tagged proteins were detected using an anti-HA antibody. The biotinylated proteins were detected using Streptavidin-HRP. Molecular mass marker in kiloDaltons is indicated on the left. The experiment was repeated three times with similar results.
(B) Biotinylation of SAG101-3FLAG by NRG1C-HA-TurboID in *A. thaliana* plants stably transformed with the two transgenes in the presence of RBA1. Immunoprecipitation was carried out with anti-FLAG beads. The 3FLAG-tagged proteins were detected using an anti-FLAG antibody. The HA-TurboID-tagged proteins were detected using an anti-HA antibody. EDS1 was detected using an anti-EDS1 antibody. The biotinylated proteins were detected using HRP-Streptavidin. Molecular mass marker in kiloDaltons is indicated on the left. The experiment was repeated twice with similar results.

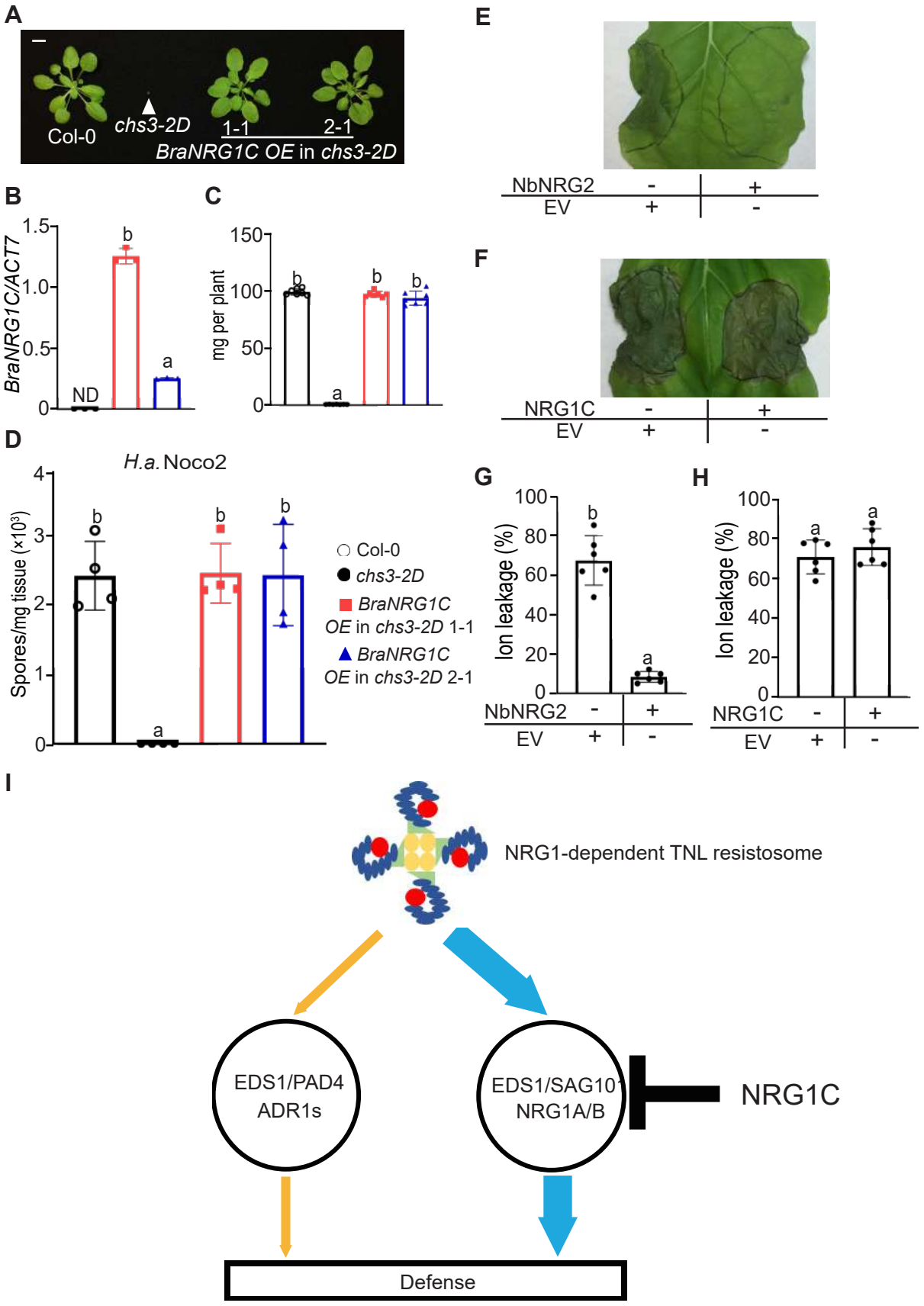

Figure 7. NRG1C-type N-terminally truncated hNLRs from canola (*Brassica napus* L. cv. Westar) and *N. benthamiana* function similarly as *A. thaliana* NRG1C.

(A) Morphology of four-week-old soil-grown plants of Col-0, *chs3-2D*, and two independent transgenic lines of *BraNRG1C OE* into *chs3-2D* background. Bar = 1cm.

(B) *BraNRG1C* gene expression in the indicated plants as determined by RT-PCR. Statistical significance is indicated by different letters ($p < 0.01$). Error bars represent means ± SE (n = 3). ND stands for Not Detectable. Two independent experiments were carried out with similar results. The color legends are included in D.

(C) Fresh weights of plants in (A). Statistical significance is indicated by different letters ($p < 0.01$). Error bars represent means ± SE (n=7). The color legends are included in D.

(D) Quantification of *H.a.* Noco2 sporulation in the indicated genotypes at 7 dpi with 10^5 spores per ml water. Statistical significance is indicated by different letters ($p < 0.01$). Error bars represent means ± SE (n=4). Three independent experiments were carried out with similar results.

(E-F) HR observation of *N. benthamiana* leaves expressing the indicated proteins at 48 hpi following the infiltration of *P.s.t.* CUCPB5500 HopQ1-1 to deliver HopQ1-1 effector. Photographs were taken at 4 dpi after *P.s.t.* CUCPB5500 HopQ1-1 infiltration.

(G-H) Ion leakage of *N. benthamiana* leaves upon *P.s.t.* CUCPB5500 HopQ1-1 infiltration under the same conditions as with E and F. Statistical significance is indicated by different letters ($p < 0.01$). Error bars represent means ± SE (n = 6). Three independent experiments were carried out with similar results.

(I) A model of two defense modules downstream of TNL activation in Arabidopsis. An effector-induced TNL resistosome with NADase activity (Horsefield et al., 2019; Ma et al., 2020; Martin et al., 2020; Tian and Li, 2020; Wan et al., 2019) signals through two parallel modules, EDS1-PAD4-ADR1s and EDS1-SAG101-NRG1A/1B to activate defense responses. N-terminally truncated hNLR NRG1C antagonizes immunity mediated by its full-length neighbors NRG1A and NRG1B to avoid aberrant activation.

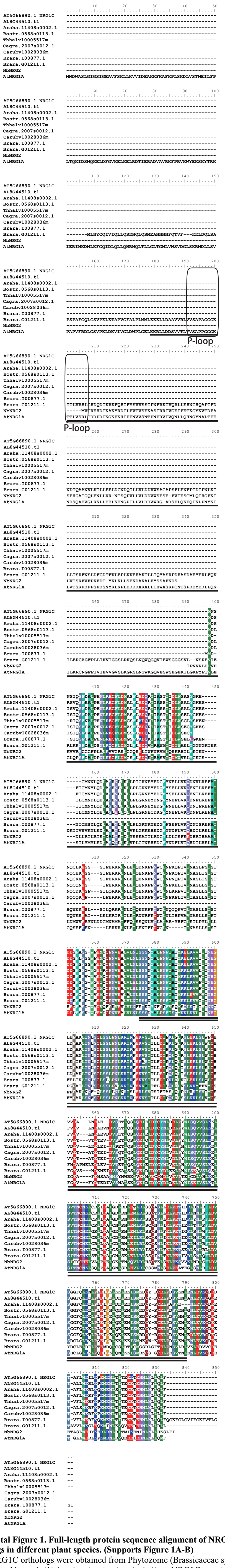

Supplemental Figure 1. Full-length protein sequence alignment of NRG1C and its orthologs in different plant species. (Supports Figure 1A-B)
Putative NRG1C orthologs were obtained from Phytozome (Brassicaceae species) and Sol Genomics Network (*N. benthamiana*) using *A. thaliana* NRG1C protein sequence as input. NB domain and LRR domain are indicated by single underline and double underline, respectively. P-loop motif is boxed in a black line.

Figure S2

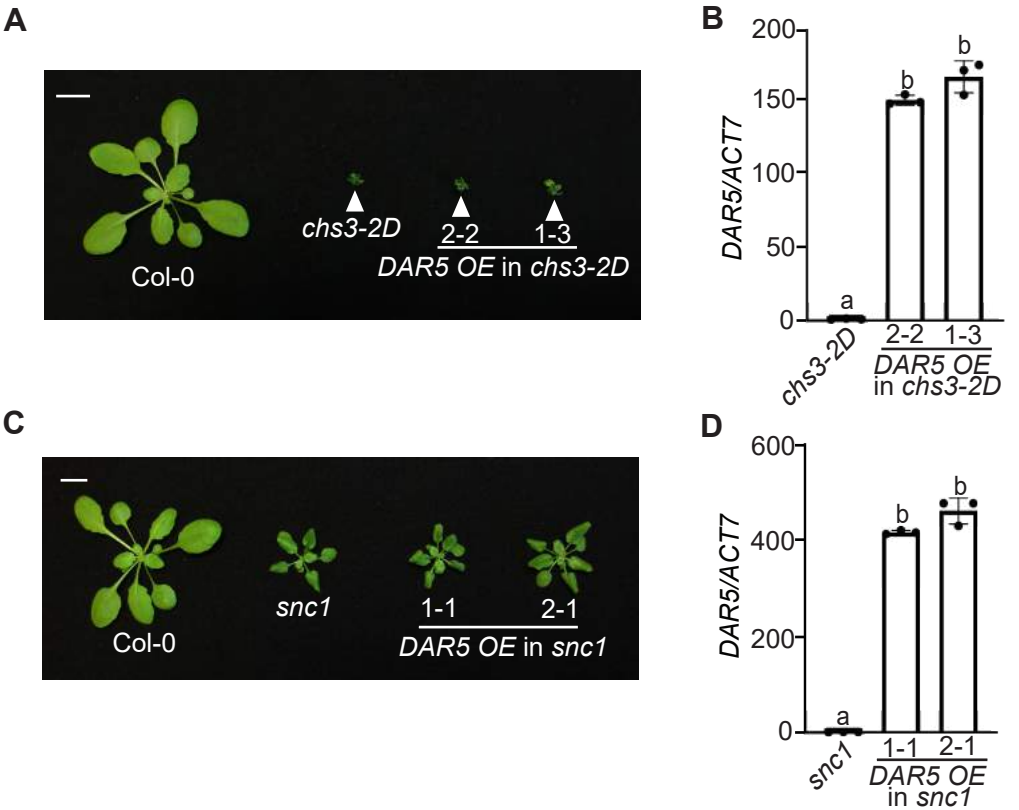

Supplemental Figure 2. DAR5 has no effect on *chs3-2D* and *snc1*-mediated autoimmunity. (Supports Figure 1D-E)

(A) Morphology of four-week-old soil-grown plants of Col-0, *chs3-2D*, and two independent transgenic lines of *DAR5 OE* into *chs3-2D* background. *OE* stands for overexpression of *DAR5*. Bar = 1cm.

(B) *DAR5* gene expression in the indicated plants as determined by RT-PCR (*chs3-2D* serves as control whose *DAR5* transcript level was set at 1.0). Statistical significance is indicated by different letters ($p < 0.01$). Error bars represent means ± SE (n = 3). Two independent experiments were carried out with similar results.

(C) Morphology of four-week-old soil-grown plants of Col-0, *snc1*, and two independent transgenic lines of *DAR5 OE* into *snc1* background. *OE* stands for overexpression of *DAR5*. Bar = 1cm.

(D) *DAR5* gene expression in the indicated plants as determined by RT-PCR (*snc1* serves as control whose *DAR5* transcript level was set at 1.0). Statistical significance is indicated by different letters ($p < 0.01$). Error bars represent means ± SE (n = 3). Two independent experiments were carried out with similar results.

Figure S3

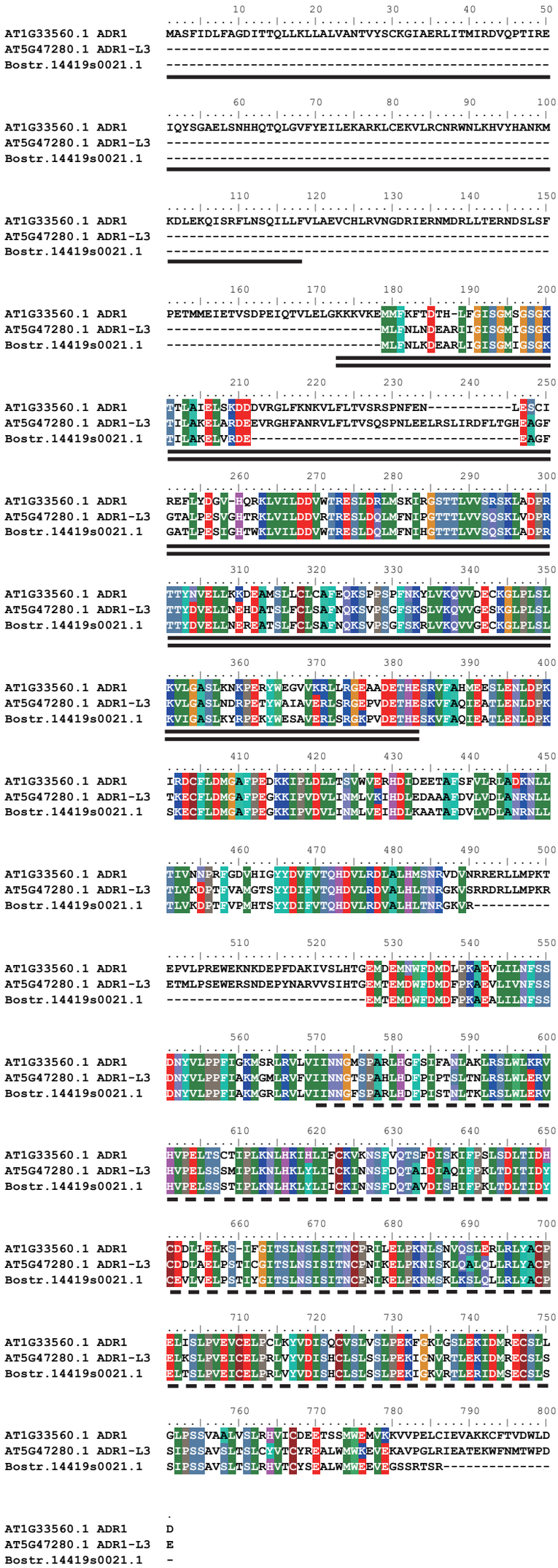

Supplemental Figure 3. Full-length protein sequence alignment of ADR1-L3 and its orthologs in different plant species. (Supports Figure 1)
Putative ADR1-L3 orthologs were obtained from Phytozome using *A. thaliana* ADR1-L3 protein sequence as input. RPW8 domain, NB domain and LRR domain are indicated by single underline, double underline and dashed underline, respectively.

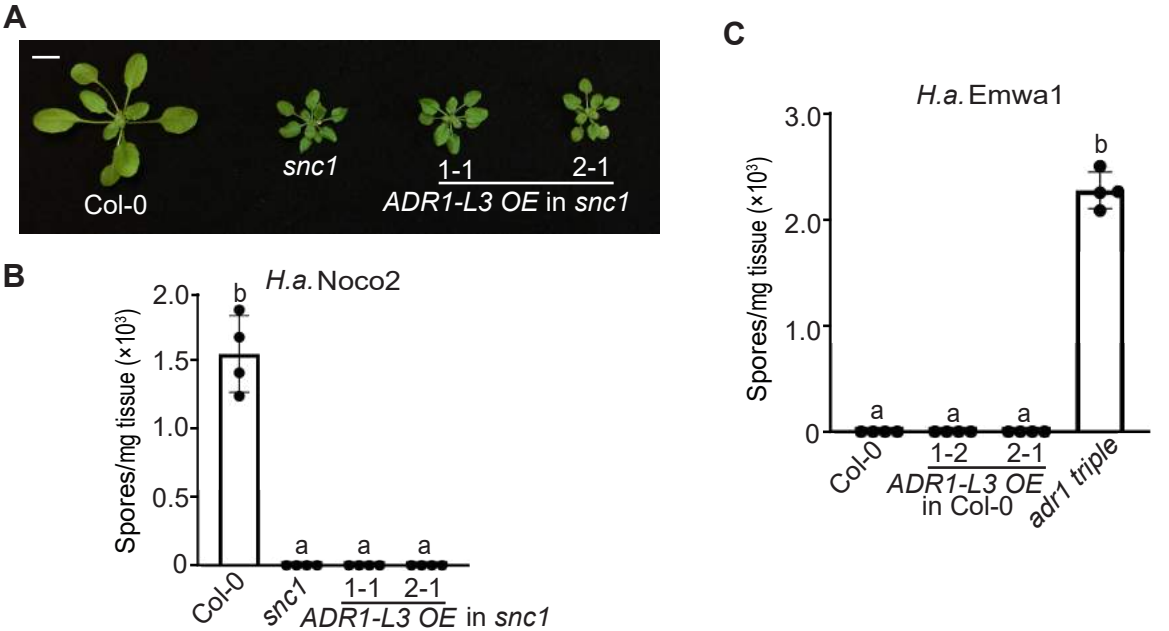

Supplemental Figure 4. No immune-related phenotypes were observed in *ADR1-L3* overexpression lines. (Supports Figure 1 and Supplemental Figure 3)

(A) Morphology of four-week-old soil-grown plants of Col-0, *snc1*, and two independent transgenic lines of *ADR1-L3 OE* into *snc1* background. *OE* stands for overexpression of *ADR1-L3*. Bar = 1cm.

(B) Quantification of *H.a.* Noco2 sporulation in the indicated genotypes at 7 dpi with 10^5 spores per ml water. Statistical significance is indicated by different letters ($p < 0.01$). Error bars represent means ± SE (n=4). Three independent experiments were carried out with similar results.

(C) Quantification of *H.a.* Emwa1 sporulation in the indicated genotypes at 7 dpi with 10^5 spores per ml water. Statistical significance is indicated by different letters ($p < 0.01$). Error bars represent means ± SE (n=4). Three independent experiments were carried out with similar results.

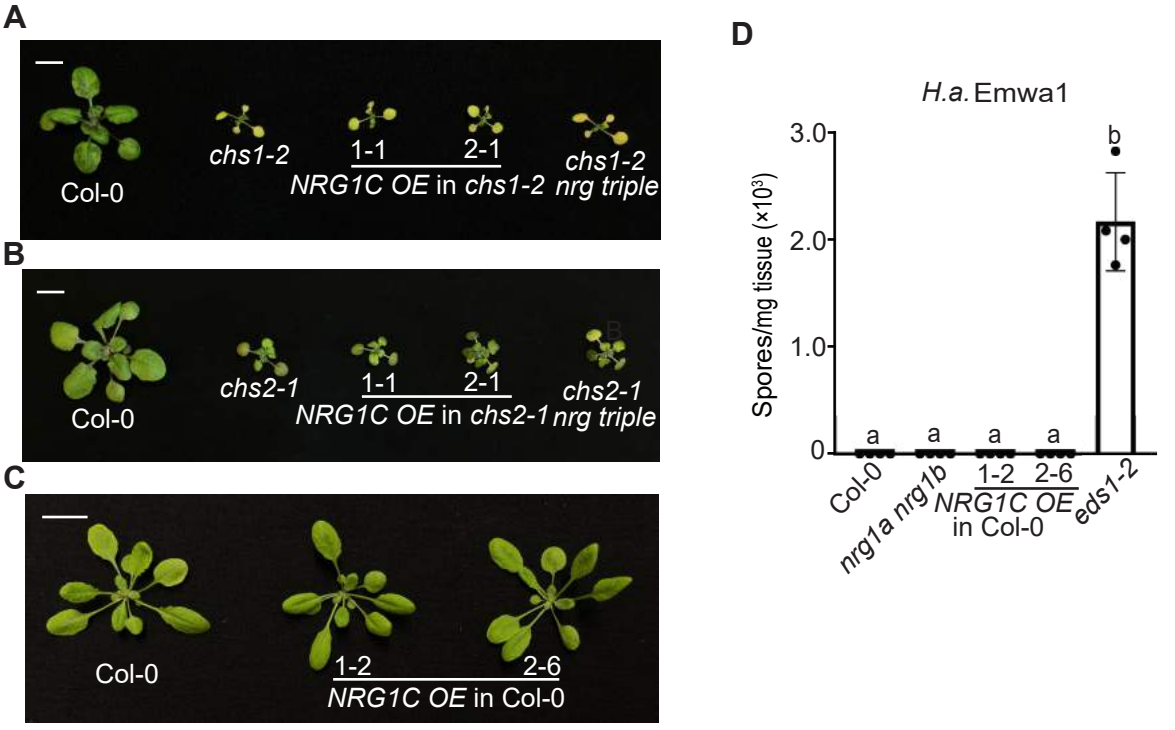

Supplemental Figure 5. Overexpression of *NRG1C* has no effect on *chs1-2* or *chs2-1*-mediated autoimmunity. (Supports Figure 2)

(A-B) Morphology of four-week-old soil-grown plants of Col-0, *chs1-2* (A), *chs2-1* (B) and two independent transgenic lines of *NRG1C OE* into *chs1-2* (A) and *chs2-1* (B) backgrounds. Plants were grown at 16 °C under long day conditions. Bar = 1cm.

(C) Morphology of four-week-old soil-grown plants of Col-0 and two independent transgenic lines of *NRG1C OE* in Col-0 background. Bar = 1cm.

(D) Quantification of *H.a.* Emwa1 sporulation in the indicated genotypes at 7 dpi with 10^5 spores per ml water. Statistical significance is indicated by different letters ($p < 0.01$). Error bars represent means ± SE (n=4). Three independent experiments were carried out with similar results.

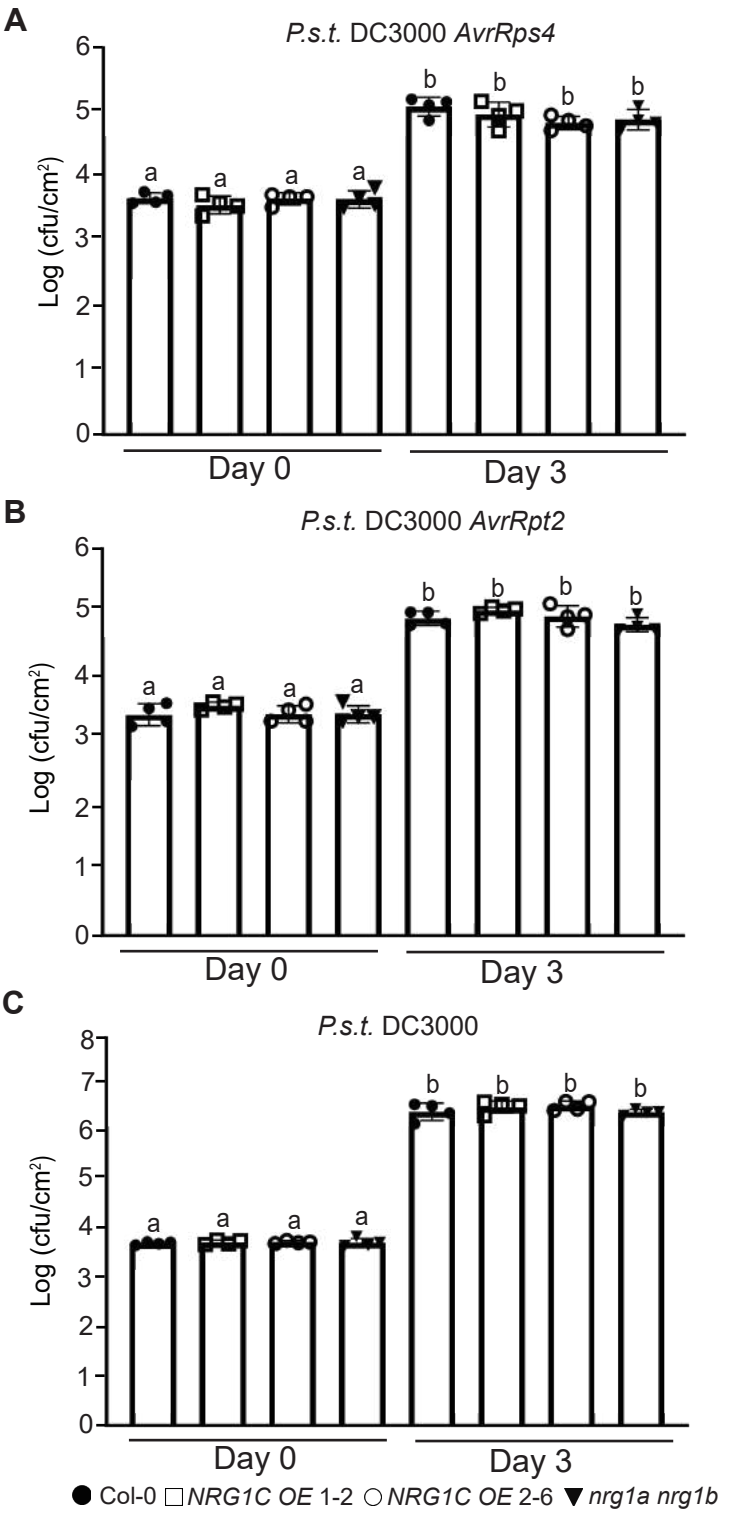

Supplemental Figure 6. NRG1C does not affect TNL RPS4 or CNL RPS2-mediated bacterial growth and basal defense. (Supports Figure 2-3)
(A-C) Growth of *P.s.t. avrRps4* (A), *avrRpt2* (B) and *P.s.t.* DC3000 (C) in four-week-old leaves of the indicated genotypes at 0 dpi and 3 dpi with bacterial inoculum of OD_{600} = 0.001. Statistical significance is indicated by different letters ($p < 0.01$). Error bars represent means ± SE (n=4). Three independent experiments were carried out with similar results.

Figure S7

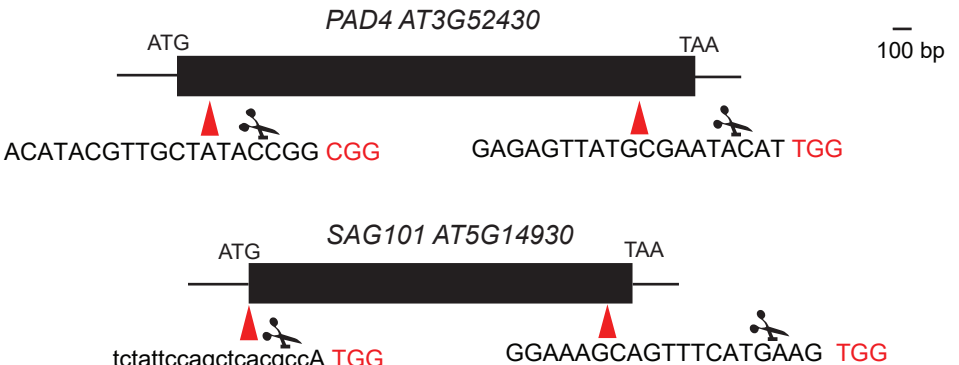

Supplemental Figure 7. Schematic description of CRISPR/Cas9 construct design to delete *PAD4* or *SAG101*. (Supports Figure 4A)
Red arrows indicate the location of two guide RNA target sites. Target sequences are shown in the below. The letters in red indicate the NGG PAM sequences. Scissors indicate where the Cas9 cut the genomic sequence.

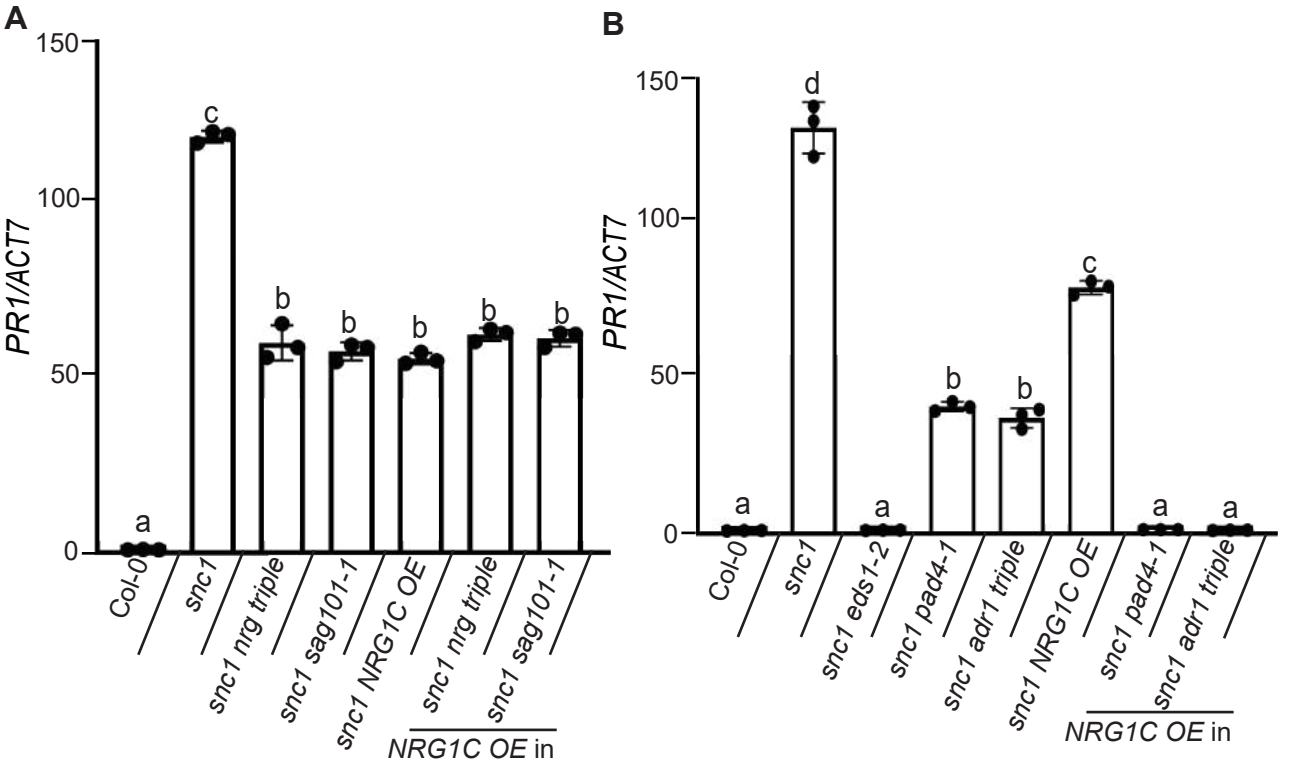

Supplemental Figure 8. NRG1C works in the same pathway with the EDS1-NRG1-SAG101 module. (Supports Figure 4C)

(A-B) *PR1* gene expression in the indicated genotypes as determined by RT-PCR (Col-0 serves as control whose *PR1* transcript level was set at 1.0). Statistical significance is indicated by different letters ($p < 0.01$). Error bars represent means ± SE (n = 3). Two independent experiments were carried out with similar results.

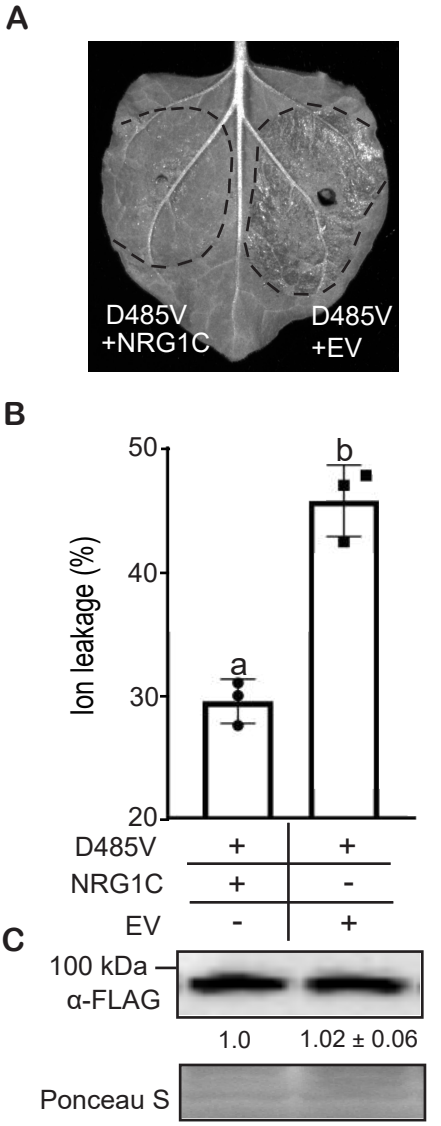

Supplemental Figure 9. NRG1C antagonizes NRG1A D485V-mediated HR. (Supports Figure 6)

(A) HR in the *N. benthamiana* leaves expressing NRG1A D485V-3FLAG and EV (Empty Vector) in the absence (right) or presence (left) of NRG1C. Photos were taken at 4 dpi. Three independent experiments were carried out with similar results.

(B) Ion leakage of *N. benthamiana* leaves upon *Agrobacterium* infiltration under the same conditions as for B. Statistical significance is indicated by different letters ($p < 0.01$). Error bars represent means ± SE (n = 3). Three independent experiments were carried out with similar results.

(C) Immunoblot analysis of protein levels of NRG1A D485V-3FLAG in leaves of B. Samples were harvest at 24 hpi, when no macroscopic HR was visible. Equal loading is shown by Ponceau S staining of a non-specific band. The numbers below represent the normalized ratio between the intensity of the protein band and the Ponceau S band ± SE (n=3). Molecular mass marker in kiloDaltons is indicated on the left.

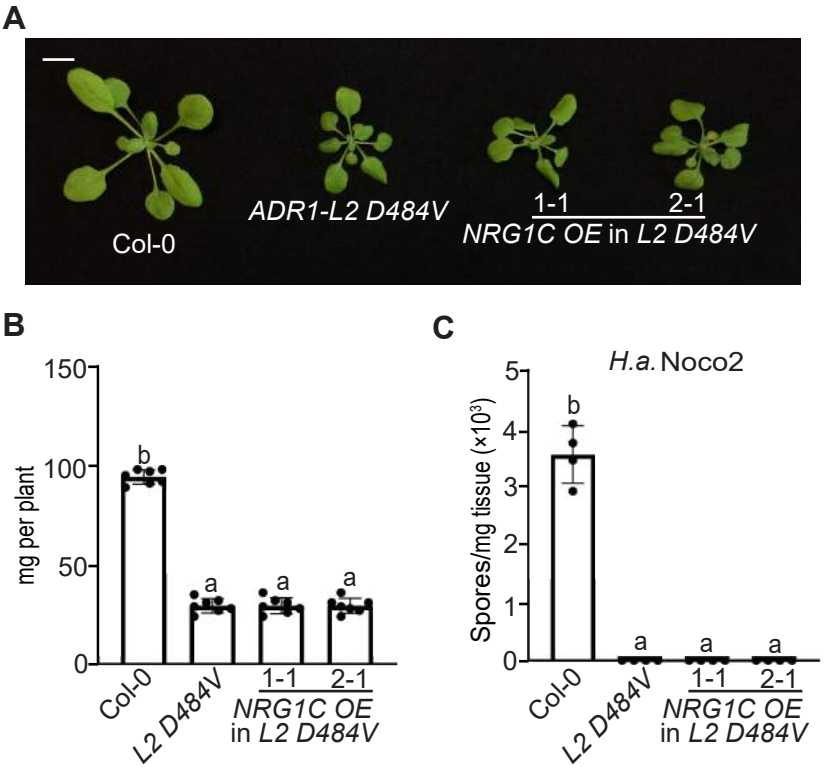

Supplemental Figure 10. NRG1C does not influence the autoimmunity of *ADR1-L2 D484V*. (Supports Figure 6)

(A) Morphology of three-week-old soil-grown plants of Col-0, *ADR1-L2 D484V*, and two independent transgenic lines of *NRG1C OE* into *ADR1-L2 D484V* background. *OE* stands for overexpression of *NRG1C*. Bar = 1cm.

(B) Fresh weights of plants in (A). Statistical significance is indicated by different letters ($p < 0.01$). Error bars represent means ± SE (n=7).

(C) Quantification of *H.a.* Noco2 sporulation in the indicated genotypes at 7 dpi with 10^5 spores per ml water. Statistical significance is indicated by different letters ($p < 0.01$). Error bars represent means ± SE (n=4). Three independent experiments were carried out with similar results.

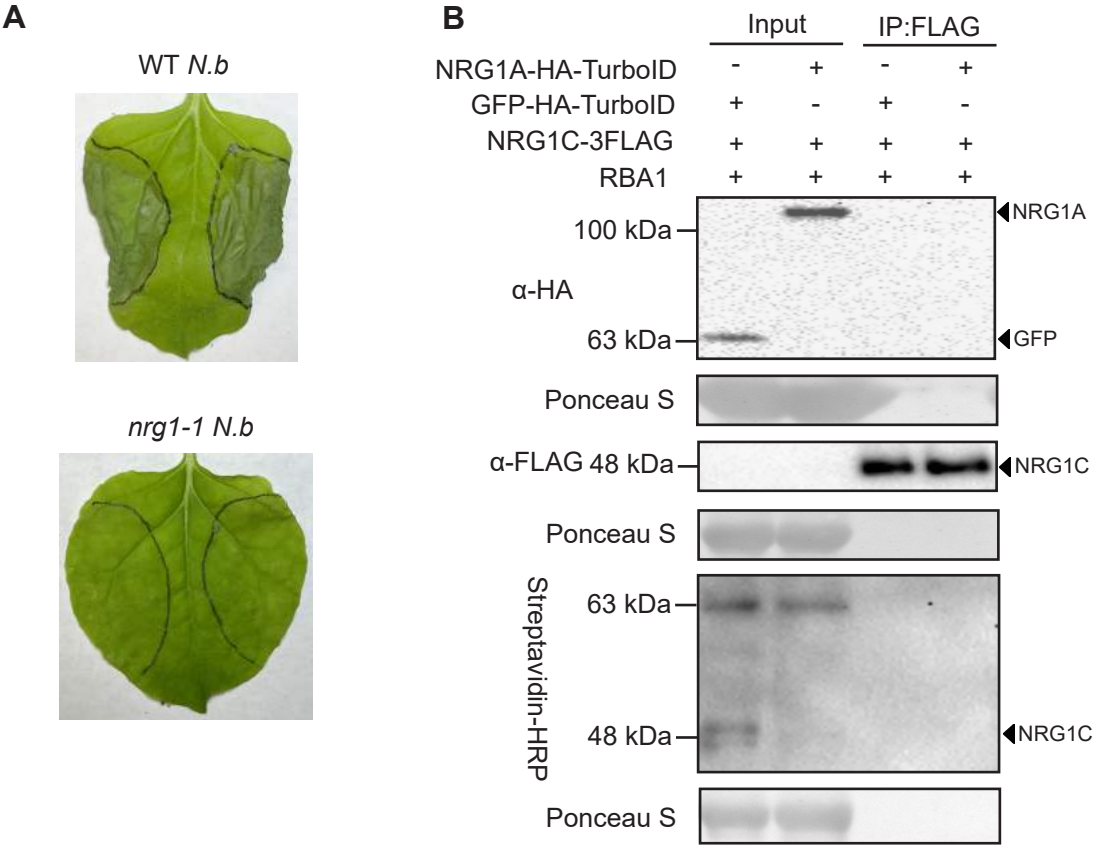

Supplemental Figure 11. NRG1C does not associate with full-length NRG1A. (Supports Figure 6)

(A) HR in the WT or *nrg1-1 N. benthamiana* leaves expressing RBA1. Photos were taken at 2 dpi. Three independent experiments were carried out with similar results.
(B) Immunoprecipitation of NRG1C-3FLAG and biotinylation of NRG1C-3FLAG by NRG1A-HATurboID in *N. benthamiana* in the presence of RBA1. Immunoprecipitation was carried out with anti-FLAG beads. The 3FLAG-tagged proteins were detected using an anti-FLAG antibody. The HA-TurboID-tagged proteins were detected using an anti-HA antibody. The biotinylated proteins were detected using Streptavidin-HRP. Molecular mass marker in kiloDaltons is indicated on the left. Three independent experiments were carried out with similar results.

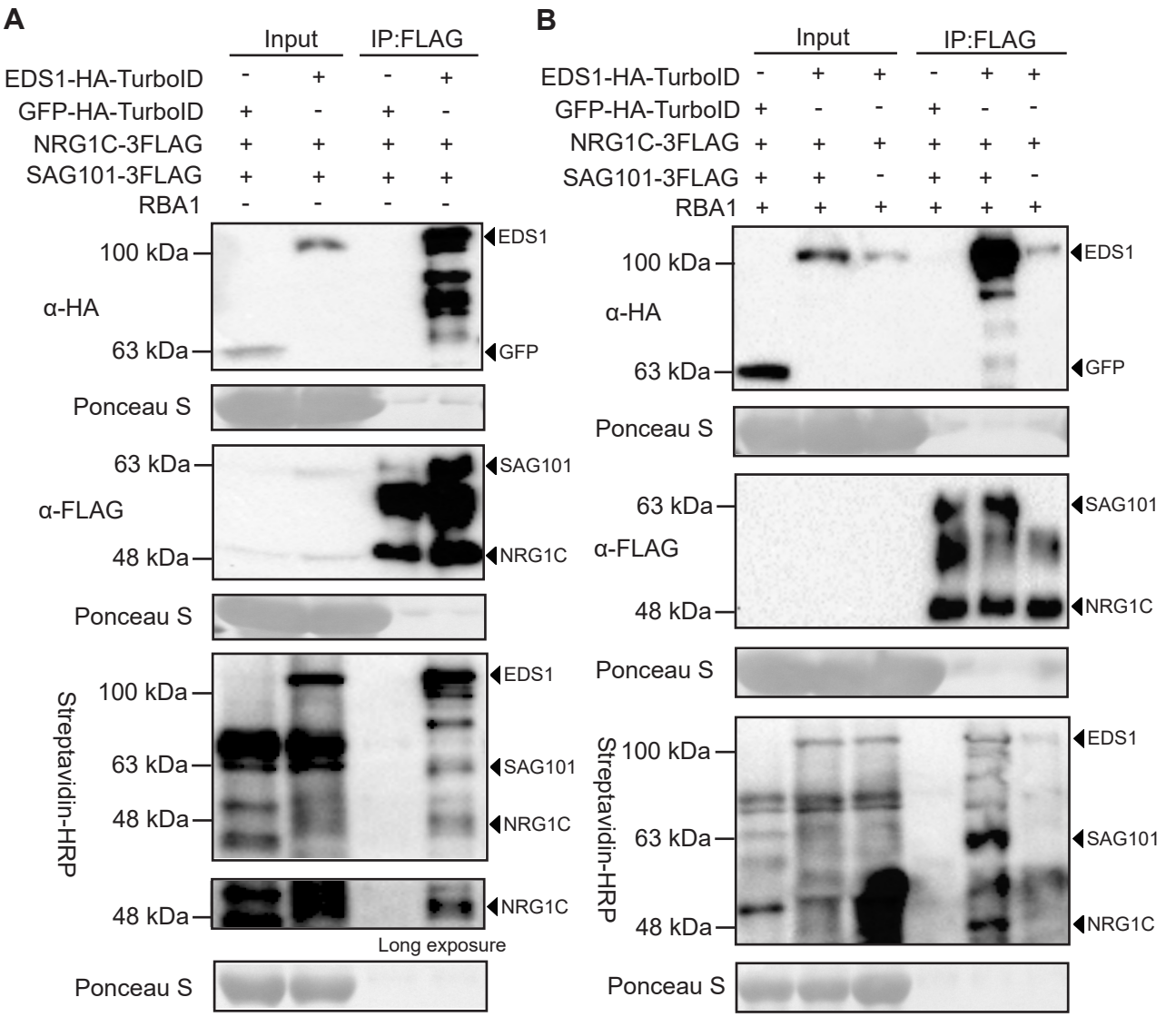

Supplemental Figure 12. The association between NRG1C with EDS1-SAG101 complex depends on TIR induction and SAG101. (Supports Figure 6)
(A) Immunoprecipitation and biotinylation of NRG1C-3FLAG and SAG101-3FLAG by EDS1-HA-TurboID in *N. benthamiana* in the absence of RBA1. Immunoprecipitation was carried out with anti-FLAG beads. The 3FLAG-tagged proteins were detected using an anti-FLAG antibody. The HA-TurboID-tagged proteins were detected using an anti-HA antibody. The biotinylated proteins were detected using Streptavidin-HRP. Molecular mass marker in kiloDaltons is indicated on the left. Three independent experiments were carried out with similar results.
(B) Immunoprecipitation and biotinylation of NRG1C-3FLAG or/and SAG101-3FLAG by EDS1-HA-TurboID in *N. benthamiana*. Immunoprecipitation was carried out with anti-FLAG beads. The 3FLAG-tagged proteins were detected using an anti-FLAG antibody. The HA-TurboID-tagged proteins were detected using an anti-HA antibody. The biotinylated proteins were detected using Streptavidin-HRP. Molecular mass marker in kiloDaltons is indicated on the left. Three independent experiments were carried out with similar results.

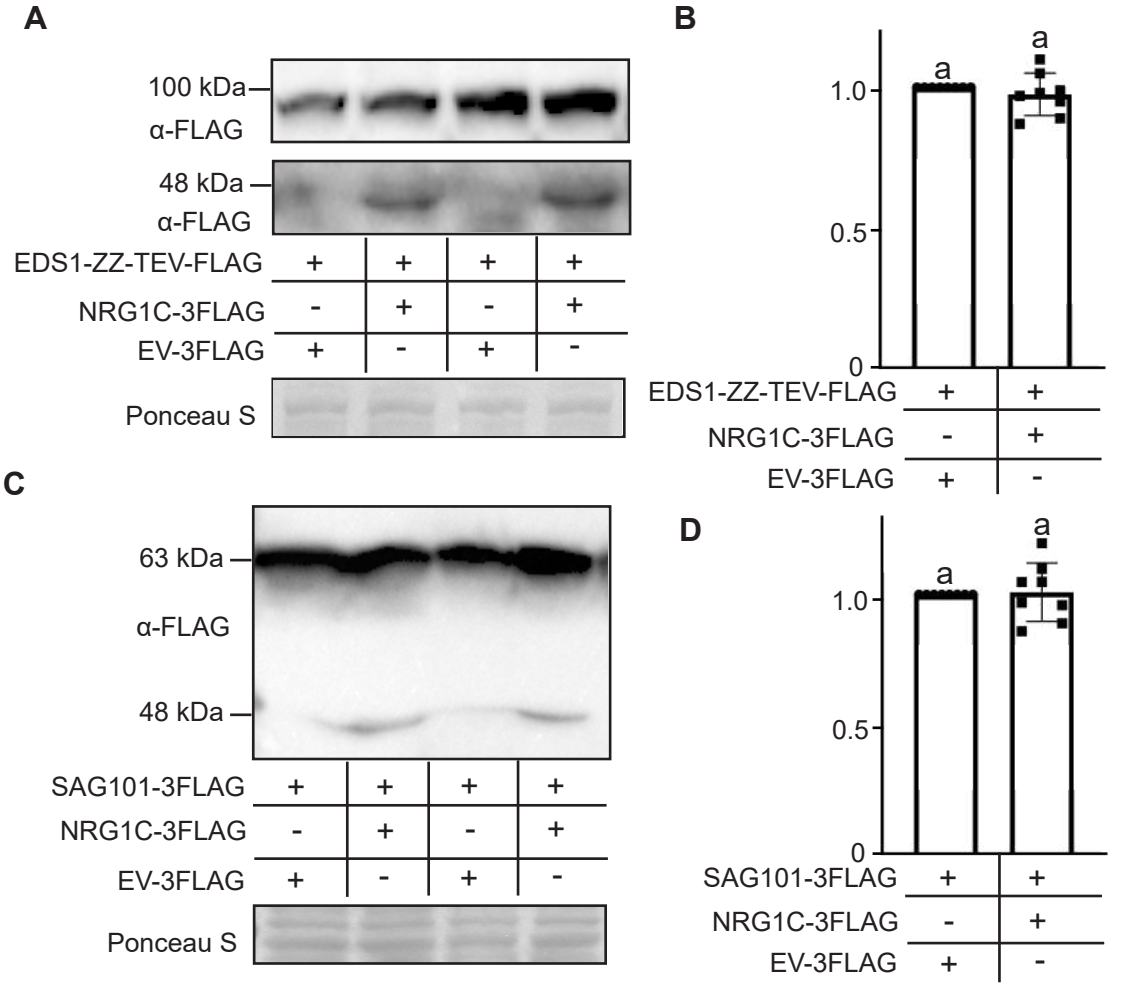

Supplemental Figure 13. Overexpression of *NRG1C* does not affect the protein levels of EDS1 and SAG101. (Supports Figure 6)

(A) Immunoblot analysis of protein levels of EDS1-ZZ-TEV-FLAG in the absence or presence of NRG1C-3FLAG. Equal loading is shown by Ponceau S staining of a non-specific band. Molecular mass marker in kiloDaltons is indicated on the left.

(B) Quantification of band intensity of (A). The numbers represent the normalized ratio between the intensity of the protein band and the Ponceau S band ± SE (n=8).

(C) Immunoblot analysis of protein levels of SAG101-3FLAG in the absence or presence of NRG1C-3FLAG. Equal loading is shown by Ponceau S staining of a non-specific band. Molecular mass marker in kiloDaltons is indicated on the left.

(D) Quantification of band intensity of C. The numbers represent the normalized ratio between the intensity of the protein band and the Ponceau S band ± SE (n=8).

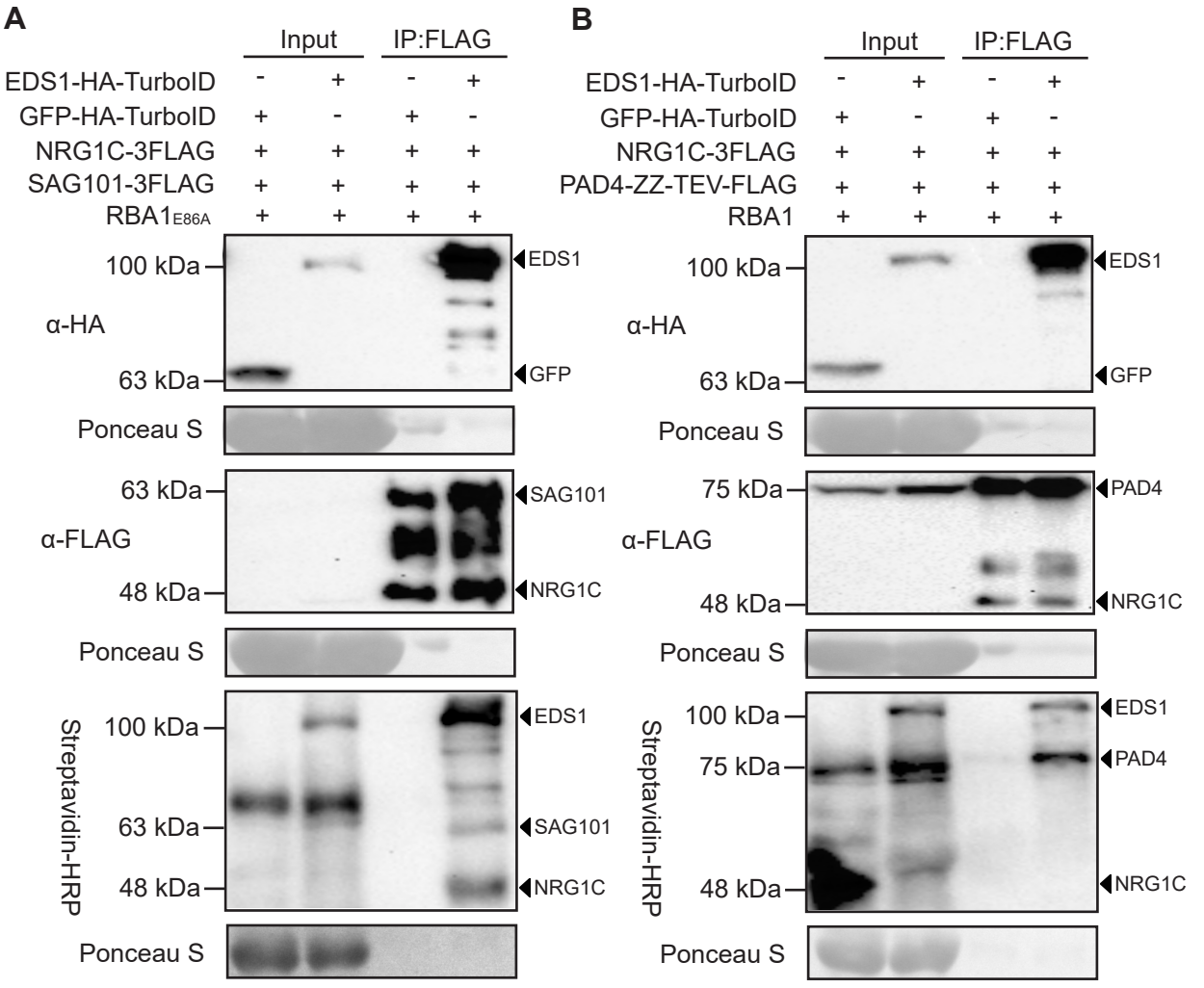

C

Treatment	-RBA1	+RBA1	+RBA1$_{E86A}$
Intensity	1.01	3.58	1.51

Supplemental Figure 14. TIR NADase enzyme activity promotes the association between NRG1C with EDS1-SAG101 complex, and NRG1C does not associate with the EDS1-PAD4 complex. (Supports Figure 6)

(A) Immunoprecipitation and biotinylation of NRG1C-3FLAG and SAG101-3FLAG by EDS1-HA-TurboID in *N. benthamiana* in the presence of RBA1$_{E86A}$. Immunoprecipitation was carried out with anti-FLAG beads. The 3FLAG-tagged proteins were detected using an anti-FLAG antibody. The HA-TurboID-tagged proteins were detected using an anti-HA antibody. The biotinylated proteins were detected using Streptavidin-HRP. Molecular mass marker in kiloDaltons is indicated on the left. Three independent experiments were carried out with similar results.

(B) Immunoprecipitation and biotinylation of NRG1C-3FLAG and PAD4-ZZ-TEV-FLAG by EDS1-HA-TurboID in *N. benthamiana* in the presence of RBA1. Immunoprecipitation was carried out with anti-FLAG beads. The ZZ-TEV-FLAG and 3FLAG-tagged proteins were detected using an anti-FLAG antibody. The HA-TurboID-tagged proteins were detected using an anti-HA antibody. The biotinylated proteins were detected using Streptavidin-HRP. Molecular mass marker in kiloDaltons is indicated on the left. Three independent experiments were carried out with similar results.

(C) The normalized ratio between the intensity of the NRG1C band and the SAG101 band in different treatments. As EDS1 constitutively associates with SAG101, SAG101 bands were used as controls.

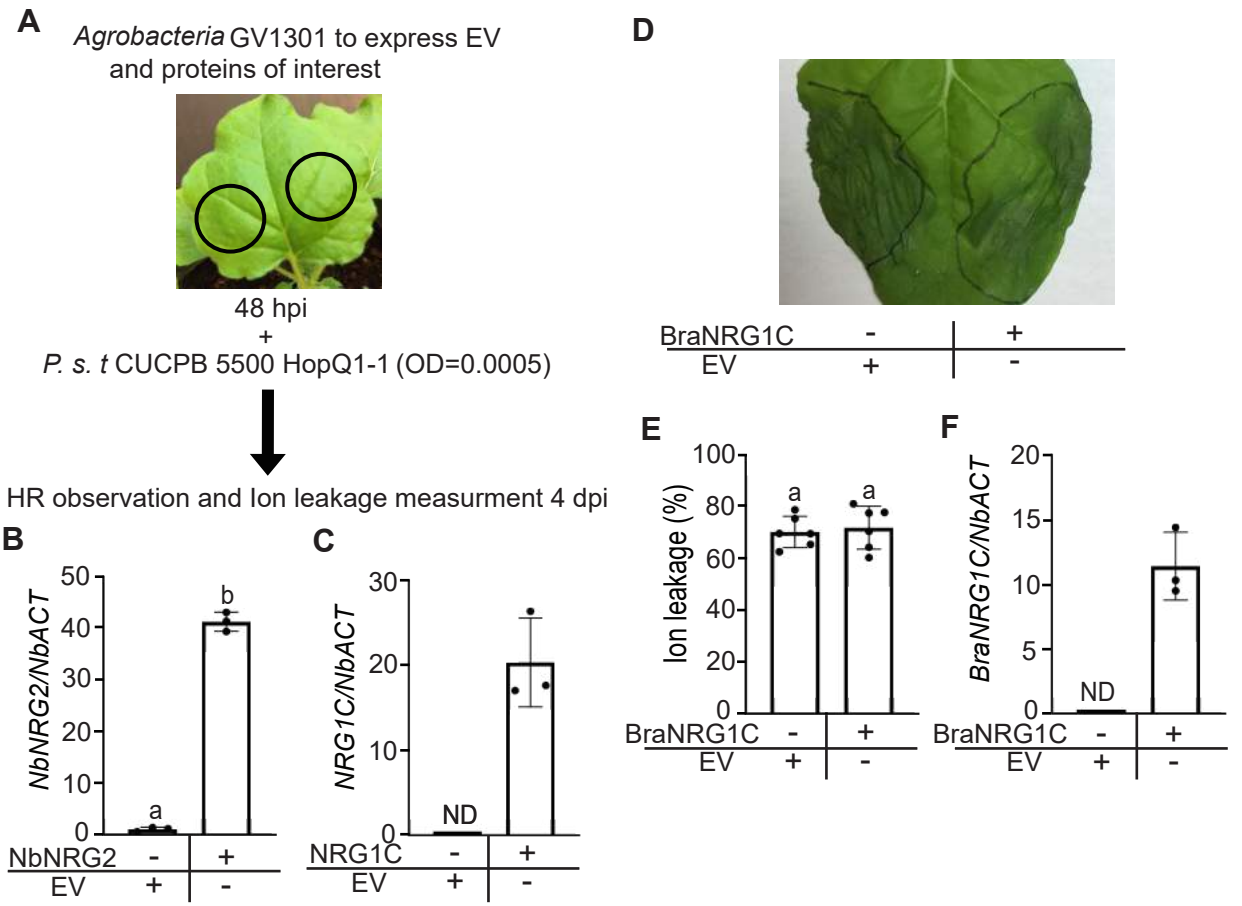

Supplemental Figure 15. Brassicaceae NRG1C ortholog does not influence HopQ1-1-mediated HR in *N. benthamiana*. (Supports Figure 7)

(A) Schematic showing *N. benthamiana* transient expression assays to test protein functionalities in HopQ1-1-dependent HR by infiltrating with *P.s.t.* CUCPB5500 HopQ1-1 (see Methods for details).

(B-C) *NbNRG2* (B) and *NRG1C* (C) genes expression in the indicated leaves as determined by RT-PCR. Statistical significance is indicated by different letters ($p < 0.01$). Error bars represent means ± SE (n = 3). The *NbNRG2* transcript level in the presence of EV treatment was set at 1.0. Two independent experiments were carried out with similar results.

(D) HR in the *N. benthamiana* leaves expressing the indicated proteins at 48 hpi following the infiltration of *P.s.t.* CUCPB5500 HopQ1-1 to deliver HopQ1-1 effector. Photographs were taken at 4 dpi after *P.s.t.* CUCPB5500 HopQ1-1 infiltration.

(E) Ion leakage of *N. benthamiana* leaves upon *P.s.t.* CUCPB5500 HopQ1-1 infiltration in the same conditions as for the photographs in D. Statistical significance is indicated by different letters ($p < 0.01$). Error bars represent means ± SE (n = 6). Three independent experiments were carried out with similar results.

(F) *BraNRG1C* gene expression in the indicated leaves as determined by RT-PCR. Error bars represent means ± SE (n = 3). Two independent experiments were carried out with similar results.

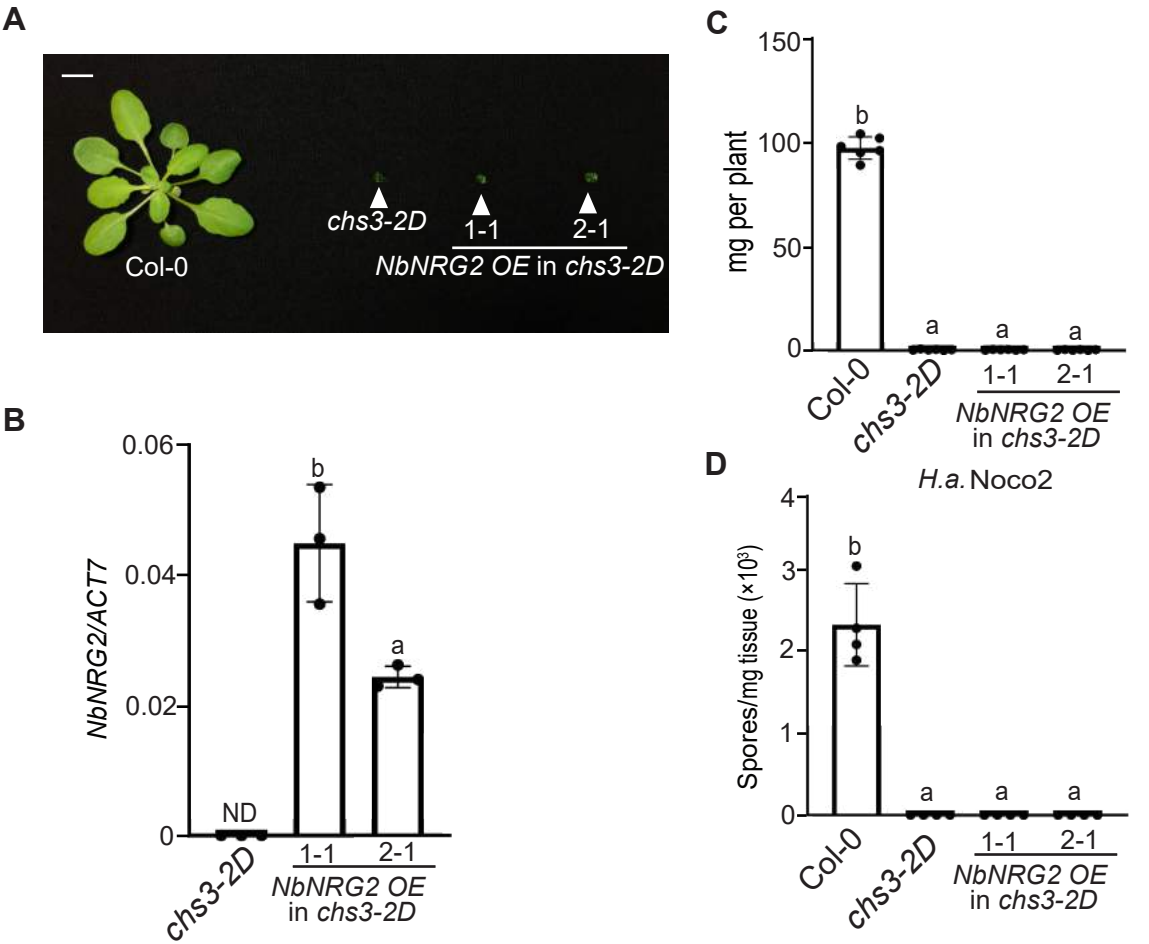

Supplemental Figure 16. NbNRG2 does not influence *chs3-2D*-mediated autoimmunity. (Supports Figure 7)

(A) Morphology of four-week-old soil-grown plants of Col-0, *chs3-2D*, and two independent transgenic lines of *NbNRG2 OE* into *chs3-2D* background. *OE* stands for overexpression of *NbNRG2*. Bar = 1cm.

(B) *NbNRG2* expression level in the indicated plants as determined by RT-PCR. Statistical significance is indicated by different letters ($p < 0.05$). Error bars represent means ± SE (n = 3). Three independent experiments were carried out with similar results.

(C) Fresh weights of plants in (A). Statistical significance is indicated by different letters ($p < 0.01$). Error bars represent means ± SE (n=6).

(D) Quantification of *H.a.* Noco2 sporulation in the indicated genotypes at 7 dpi with 10^5 spores per ml water. Statistical significance is indicated by different letters ($p < 0.01$). Error bars represent means ± SE (n=4). Three independent experiments were carried out with similar results.

Supplemental Table 1. The genome arrangement of NRG1C in plant species.

Species	*NRG1C* gene arrangement
Arabidopsis thaliana	
Arabidopsis lyrata	
Arabidopsis halleri	
Boechera stricta	
Capsella grandiflora	
Capsella rubella	
Eutrema salsugineum	
Brassica rapa	

Arrows in tandem indicate tandemly arranged genes, while arrows in rows indicate randomly assorted genes on different scaffolds. All sequences were obtained from Phytozome. *A. thaliana* (*AT5G66910*, *AT5G66900*, *AT5G66890*); *Arabidopsis lyrate* (*AL8G44490*, *AL8G44500*, *AL8G44510*); *Arabidopsis haller* (*Araha.11408s0003.1*, *Araha.11408s0002.1*); *Boechera stricta* (*Bostr.27102s0001.1*; *Bostr.0568s0113.1*); *Capsella grandiflora* (*Cagra.2007s0011.1*, *Cagra.2007s0012.1*); *Capsella rubella* (*Carubv 10027991m*, *Carubv10028036m*); *Eutrema salsugineum* (*Thhalv10003662m*, *Thhalv10005443m*, *Thhalv10005517m*; *Thhalv10020099m*); *Brassica rapa* (*Brara.I00877.1*, *Brara.I00876.1*; *Brara.G01212.1*, *Brara.G01211.1*; *Brara.B03562.1*; *Brara.F02778.1*). All truncated NRG1C orthologs are labeled with yellow arrows. Orange arrow indicates *Brara.*G01211.1.

Supplemental Table 2. The genome arrangement of *NL* truncated genes in *Arabidopsis*.

NLs Cluster	Genes arrangement
1	4G19060 4G19050
2	5G45440 .... 5G45490 .... 5G45510 5G45520
3	1G61310 1G61300
4	5G38340 5G38344 5G38350
5	4G09360 .... 4G09420 4G09430

Arrows in tandem indicate tandemly arranged genes. Dashed line indicates two genes are clustered, but not tandemly arranged. Gene codes are shown under the arrows. Orange, yellow, black, and blue arrows indicate CN, NL, full-length NLR, TIR-only proteins, respectively.

Supplemental Table 3. The list of primers used in this study.

Name	Sequence	Purpose
NRG1C-KpnI-F	gcgcggtaccATG AATTCGAATTCGATTCA	To generate pCambia 1305 NRG1C
NRG1C-SpeI-R	gactagtTTAAAACAGTTGAAGCAAGTTGA	
NRG1C-KpnI-F	gcgcggtaccATG AATTCGAATTCGATTCA	To generate pCambia 1300 NRG1C-3FLAG
NRG1C-SpeI(ns)-R	gactagtAAACAGTTGAAGCAAGTTGAG	
1C-Y71ST-F	atagGAGAAATGAGTAGGAAGATGGTTTCTAC	To generate pCambia 1305 NRG1C T71STOP
1C-Y71ST-R	GTAGAAACCATCTTCCTACTCATTTCTCCTAT	
DAR5-SfiI-F	CCCGGCCGTCAAGGCCATGCCGATCTCGGATGT	To generate pHan DAR5
DAR5-SfiI-R	GCCGGCCCATGAGGCCTTACCTCCGGCGAAGAAT	
SAG101-CK-F	gagtaacaaattcgtcttggag	To genotype SAG101 CRISPR allele
SAG101-CK-R	CTAAGAGTTGTTGCGATTGATG	
SAG101-homo-R	GAATGATGGGTTGTTCTCG	
PAD4-checking-F	ccgattacataggatcacatgc	To genotype PAD4 CRISPR allele
PAD4-checking-R	CACCATCACACTACATGTTGG	
PAD4-homo-F	CAGATACGCGAGCACAAC	
NRG1C-RT-F	CTTCCTATTGGGAGAAATGAG	NRG1C RT primers
NRG1C-RT-R	CACAACCTTCAATTCCTTC	
DAR5-RT-F	CTCCTCTTAGCATGTGTGGT	DAR5 RT primers
DAR5-RT-R	CCATCAGCTTCATGAACAGG	
NRG1-KpnI-F	gcgcggtaccCATGAACGATTGGGCTAGTTTG	To generate pBNRG1AHATurboID
NRG1-SpeI(NS)-R	gactagtcAAACATTTGAAGCAAGTTCAGGT	
SAG101-KpnI-F	gcgcggtaccATGGAGTCTTCTTCTTCACT	

SAG101-BamHI(NS)-R	cgcggatccTTGTGACTTACCATAACTCTCG	To generate pCambia SAG101-3FLAG
Bra877-DraIII-F	cggcggCACTCAGTGATGATGGATTCGATCCAAAG	To generate pBBraNRG1C
Bra877-DraIII-R	cggcggCACATGGTGTCATATACTTCCTAATGTTACAAA	
Bra877-RT-F	TGCCTCCCACAATCTTC	BraNRG1C RT primers
Bra877-RT-R	GCAAATTCTCTCGAGATGTTG	
NRG2-KpnI-F	gcgcggtaccatggtttgtcgagagcatga	To generate pBNbNRG2
NRG2-SpeI-R	GGACTAGTTCAGATAAATAACGATTTATGCAGC	
NRG2-RT-F	tgtgcgacttgatcttgttc	NbNRG2 RT primers
NRG2-RT-R	GCAGCAGCACATCACTCT	
PAD4_BsF	ATATATGGTCTCGATTGACATACGTTGCTATACCGGGTT	To generate PAD4 CRISPR
PAD4_F0	TGACATACGTTGCTATACCGGGTTTTAGAGCTAGAAATAGC	
PAD4_R0	AACATGTATTCGCATAACTCTCCAATCTCTTAGTCGACTCTAC	
PAD4_BsR	ATTATTGGTCTCGAAACATGTATTCGCATAACTCTCC	
SAG101_BsF	ATATATGGTCTCGATTGtctattccagctcacgccAGTT	To generate SAG101 CRISPR
SAG101_F0	TGtctattccagctcacgccAGTTTTAGAGCTAGAAATAGC	
SAG101_R0	AACCTTCATGAAACTGCTTTCCCAATCTCTTAGTCGACTCTAC	
SAG101_BsR	ATTATTGGTCTCGAAACCTTCATGAAACTGCTTTCCC	

Parsed Citations

Adachi, H., Contreras, M.P., Harant, A., Wu, C.H., Derevnina, L., Sakai, T., Duggan, C., Moratto, E., Bozkurt, T.O., Maqbool, A., et al. (2019). An N-terminal motif in NLR immune receptors is functionally conserved across distantly related plant species. Elife 8.
Google Scholar: Author Only Title Only Author and Title

Andolfo, G., Villano, C., Errico, A., Frusciante, L., Carputo, D., Aversano, R., and Ercolano, M.R. (2019). Inferring RPW8-NLRs's evolution patterns in seed plants: case study in Vitis vinifera. Planta 251:32.
Google Scholar: Author Only Title Only Author and Title

Baggs, E., Dagdas, G., and Krasileva, K.V. (2017). NLR diversity, helpers and integrated domains: making sense of the NLR IDentity. Curr Opin Plant Biol 38:59-67.
Google Scholar: Author Only Title Only Author and Title

Bai, J., Pennill, L.A., Ning, J., Lee, S.W., Ramalingam, J., Webb, C.A., Zhao, B., Sun, Q., Nelson, J.C., Leach, J.E., et al. (2002). Diversity in nucleotide binding site-leucine-rich repeat genes in cereals. Genome Res 12:1871-1884.
Google Scholar: Author Only Title Only Author and Title

Barragan, A.C., Collenberg, M., Wang, J., Lee, R.R.Q., Cher, W.Y., Rabanal, F.A., Ashkenazy, H., Weigel, D., and Chae, E. (2020). A truncated singleton NLR causes hybrid necrosis in Arabidopsis thaliana. Mol Biol Evol.
Google Scholar: Author Only Title Only Author and Title

Bonardi, V., Tang, S., Stallmann, A., Roberts, M., Cherkis, K., and Dangl, J.L. (2011). Expanded functions for a family of plant intracellular immune receptors beyond specific recognition of pathogen effectors. Proc Natl Acad Sci U S A 108:16463-16468.
Google Scholar: Author Only Title Only Author and Title

Burns, K., Janssens, S., Brissoni, B., Olivos, N., Beyaert, R., and Tschopp, J. (2003). Inhibition of interleukin 1 receptor/Toll-like receptor signaling through the alternatively spliced, short form of MyD88 is due to its failure to recruit IRAK-4. J Exp Med 197:263-268.
Google Scholar: Author Only Title Only Author and Title

Castel, B., Ngou, P.M., Cevik, V., Redkar, A., Kim, D.S., Yang, Y., Ding, P., and Jones, J.D.G. (2019). Diverse NLR immune receptors activate defence via the RPW8-NLR NRG1. New Phytol 222:966-980.
Google Scholar: Author Only Title Only Author and Title

Cheng, Y.T., Li, Y., Huang, S., Huang, Y., Dong, X., Zhang, Y., and Li, X. (2011). Stability of plant immune-receptor resistance proteins is controlled by SKP1-CULLIN1-F-box (SCF)-mediated protein degradation. Proc Natl Acad Sci U S A 108:14694-14699.
Google Scholar: Author Only Title Only Author and Title

Clough, S.J., and Bent, A.F. (1998). Floral dip: a simplified method for Agrobacterium-mediated transformation of Arabidopsis thaliana. Plant J 16:735-743.
Google Scholar: Author Only Title Only Author and Title

Collier, S.M., Hamel, L.P., and Moffett, P. (2011). Cell death mediated by the N-terminal domains of a unique and highly conserved class of NB-LRR protein. Mol Plant Microbe Interact 24:918-931.
Google Scholar: Author Only Title Only Author and Title

Couto, D., and Zipfel, C. (2016). Regulation of pattern recognition receptor signalling in plants. Nat Rev Immunol 16:537-552.
Google Scholar: Author Only Title Only Author and Title

Cui, H., Tsuda, K., and Parker, J.E. (2015). Effector-triggered immunity: from pathogen perception to robust defense. Annu Rev Plant Biol 66:487-511.
Google Scholar: Author Only Title Only Author and Title

Dong, O.X., Tong, M., Bonardi, V., El Kasmi, F., Woloshen, V., Wünsch, L.K., Dangl, J.L., and Li, X. (2016). TNL-mediated immunity in Arabidopsis requires complex regulation of the redundant ADR1 gene family. New Phytol 210:960-973.
Google Scholar: Author Only Title Only Author and Title

Feys, B.J., Moisan, L.J., Newman, M.A., and Parker, J.E. (2001). Direct interaction between the Arabidopsis disease resistance signaling proteins, EDS1 and PAD4. EMBO J 20:5400-5411.
Google Scholar: Author Only Title Only Author and Title

Feys, B.J., Wiermer, M., Bhat, R.A., Moisan, L.J., Medina-Escobar, N., Neu, C., Cabral, A., and Parker, J.E. (2005). Arabidopsis SENESCENCE-ASSOCIATED GENE101 stabilizes and signals within an ENHANCED DISEASE SUSCEPTIBILITY1 complex in plant innate immunity. Plant Cell 17:2601-2613.
Google Scholar: Author Only Title Only Author and Title

Gabriëls, S.H., Takken, F.L., Vossen, J.H., de Jong, C.F., Liu, Q., Turk, S.C., Wachowski, L.K., Peters, J., Witsenboer, H.M., de Wit, P.J., et al. (2006). CDNA-AFLP combined with functional analysis reveals novel genes involved in the hypersensitive response. Mol Plant Microbe Interact 19:567-576.
Google Scholar: Author Only Title Only Author and Title

Gabriëls, S.H., Vossen, J.H., Ekengren, S.K., van Ooijen, G., Abd-El-Haliem, A.M., van den Berg, G.C., Rainey, D.Y., Martin, G.B., Takken, F.L., de Wit, P.J., et al. (2007). An NB-LRR protein required for HR signalling mediated by both extra- and intracellular

resistance proteins. Plant J 50:14-28.
Google Scholar: Author Only Title Only Author and Title

Gao, Y., Wang, W., Zhang, T., Gong, Z., Zhao, H., and Han, G.Z. (2018). Out of Water: The Origin and Early Diversification of Plant. Plant Physiol 177:82-89.
Google Scholar: Author Only Title Only Author and Title

Guo, Y.L., Fitz, J., Schneeberger, K., Ossowski, S., Cao, J., and Weigel, D. (2011). Genome-wide comparison of nucleotide-binding site-leucine-rich repeat-encoding genes in Arabidopsis. Plant Physiol 157:757-769.
Google Scholar: Author Only Title Only Author and Title

Horsefield, S., Burdett, H., Zhang, X., Manik, M.K., Shi, Y., Chen, J., Qi, T., Gilley, J., Lai, J.S., Rank, M.X., et al. (2019). NAD. Science 365:793-799.
Google Scholar: Author Only Title Only Author and Title

Huang, X., Li, J., Bao, F., Zhang, X., and Yang, S. (2010). A gain-of-function mutation in the Arabidopsis disease resistance gene RPP4 confers sensitivity to low temperature. Plant Physiol 154:796-809.
Google Scholar: Author Only Title Only Author and Title

Jacob, F., Vernaldi, S., and Maekawa, T. (2013). Evolution and Conservation of Plant NLR Functions. Front Immunol 4:297.
Google Scholar: Author Only Title Only Author and Title

Jones, J.D., Vance, R.E., and Dangl, J.L. (2016). Intracellular innate immune surveillance devices in plants and animals. Science 354.
Google Scholar: Author Only Title Only Author and Title

Jubic, L.M., Saile, S., Furzer, O.J., El Kasmi, F., and Dangl, J.L. (2019). Help wanted: helper NLRs and plant immune responses. Curr Opin Plant Biol 50:82-94.
Google Scholar: Author Only Title Only Author and Title

Krasileva, K.V. (2019). The role of transposable elements and DNA damage repair mechanisms in gene duplications and gene fusions in plant genomes. Curr Opin Plant Biol 48:18-25.
Google Scholar: Author Only Title Only Author and Title

Kvitko, B.H., Park, D.H., Velásquez, A.C., Wei, C.F., Russell, A.B., Martin, G.B., Schneider, D.J., and Collmer, A. (2009). Deletions in the repertoire of Pseudomonas syringae pv. tomato DC3000 type III secretion effector genes reveal functional overlap among effectors. PLoS Pathog 5:e1000388.
Google Scholar: Author Only Title Only Author and Title

Lakatos, L., Szittya, G., Silhavy, D., and Burgyán, J. (2004). Molecular mechanism of RNA silencing suppression mediated by p19 protein of tombusviruses. EMBO J 23:876-884.
Google Scholar: Author Only Title Only Author and Title

Lapin, D., Kovacova, V., Sun, X., Dongus, J.A., Bhandari, D., von Born, P., Bautor, J., Guarneri, N., Rzemieniewski, J., Stuttmann, J., et al. (2019). A Coevolved EDS1-SAG101-NRG1 Module Mediates Cell Death Signaling by TIR-Domain Immune Receptors. Plant Cell 31:2430-2455.
Google Scholar: Author Only Title Only Author and Title

Lee, R.R.Q., and Chae, E. (2020). Variation Patterns of NLR Clusters in. Plant Commun 1:100089.
Google Scholar: Author Only Title Only Author and Title

Li, X., Clarke, J.D., Zhang, Y., and Dong, X. (2001). Activation of an EDS1-mediated R-gene pathway in the snc1 mutant leads to constitutive, NPR1-independent pathogen resistance. Mol Plant Microbe Interact 14:1131-1139.
Google Scholar: Author Only Title Only Author and Title

Liang, W., van Wersch, S., Tong, M., and Li, X. (2019). TIR-NB-LRR immune receptor SOC3 pairs with truncated TIR-NB protein CHS1 or TN2 to monitor the homeostasis of E3 ligase SAUL1. New Phytol 221:2054-2066.
Google Scholar: Author Only Title Only Author and Title

Liu, N., Hake, K., Wang, W., Zhao, T., Romeis, T., and Tang, D. (2017). CALCIUM-DEPENDENT PROTEIN KINASE5 Associates with the Truncated NLR Protein TIR-NBS2 to Contribute to. Plant Cell 29:746-759.
Google Scholar: Author Only Title Only Author and Title

Lu, X., Kracher, B., Saur, I.M., Bauer, S., Ellwood, S.R., Wise, R., Yaeno, T., Maekawa, T., and Schulze-Lefert, P. (2016). Allelic barley MLA immune receptors recognize sequence-unrelated avirulence effectors of the powdery mildew pathogen. Proc Natl Acad Sci U S A 113:E6486-E6495.
Google Scholar: Author Only Title Only Author and Title

Ma, S., Lapin, D., Liu, L., Sun, Y., Song, W., Zhang, X., Logemann, E., Yu, D., Wang, J., Jirschitzka, J., et al. (2020). Direct pathogen-induced assembly of an NLR immune receptor complex to form a holoenzyme. Science 370.
Google Scholar: Author Only Title Only Author and Title

Mago, R., Zhang, P., Vautrin, S., Šimková, H., Bansal, U., Luo, M.C., Rouse, M., Karaoglu, H., Periyannan, S., Kolmer, J., et al. (2015). The wheat Sr50 gene reveals rich diversity at a cereal disease resistance locus. Nat Plants 1:15186.
Google Scholar: Author Only Title Only Author and Title

Marone, D., Russo, M.A., Laidò, G., De Leonardis, A.M., and Mastrangelo, A.M. (2013). Plant nucleotide binding site-leucine-rich repeat (NBS-LRR) genes: active guardians in host defense responses. Int J Mol Sci 14:7302-7326.
Google Scholar: Author Only Title Only Author and Title

Martin, R., Qi, T., Zhang, H., Liu, F., King, M., Toth, C., Nogales, E., and Staskawicz, B.J. (2020). Structure of the activated ROQ1 resistosome directly recognizing the pathogen effector XopQ. Science 370.
Google Scholar: Author Only Title Only Author and Title

Meyers, B.C., Kozik, A., Griego, A., Kuang, H., and Michelmore, R.W. (2003). Genome-wide analysis of NBS-LRR-encoding genes in Arabidopsis. Plant Cell 15:809-834.
Google Scholar: Author Only Title Only Author and Title

Meyers, B.C., Morgante, M., and Michelmore, R.W. (2002). TIR-X and TIR-NBS proteins: two new families related to disease resistance TIR-NBS-LRR proteins encoded in Arabidopsis and other plant genomes. Plant J 32:77-92.
Google Scholar: Author Only Title Only Author and Title

Michelmore, R.W., and Meyers, B.C. (1998). Clusters of resistance genes in plants evolve by divergent selection and a birth-and-death process. Genome Res 8:1113-1130.
Google Scholar: Author Only Title Only Author and Title

Nandety, R.S., Caplan, J.L., Cavanaugh, K., Perroud, B., Wroblewski, T., Michelmore, R.W., and Meyers, B.C. (2013). The role of TIR-NBS and TIR-X proteins in plant basal defense responses. Plant Physiol 162:1459-1472.
Google Scholar: Author Only Title Only Author and Title

Nishimura, M.T., Anderson, R.G., Cherkis, K.A., Law, T.F., Liu, Q.L., Machius, M., Nimchuk, Z.L., Yang, L., Chung, E.H., El Kasmi, F., et al. (2017). TIR-only protein RBA1 recognizes a pathogen effector to regulate cell death in. Proc Natl Acad Sci U S A 114:E2053-E2062.
Google Scholar: Author Only Title Only Author and Title

Padmanabhan, M., Cournoyer, P., and Dinesh-Kumar, S.P. (2009). The leucine-rich repeat domain in plant innate immunity: a wealth of possibilities. Cell Microbiol 11:191-198.
Google Scholar: Author Only Title Only Author and Title

Peart, J.R., Mestre, P., Lu, R., Malcuit, I., and Baulcombe, D.C. (2005). NRG1, a CC-NB-LRR protein, together with N, a TIR-NB-LRR protein, mediates resistance against tobacco mosaic virus. Curr Biol 15:968-973.
Google Scholar: Author Only Title Only Author and Title

Qi, T., Seong, K., Thomazella, D.P.T., Kim, J.R., Pham, J., Seo, E., Cho, M.J., Schultink, A., and Staskawicz, B.J. (2018). NRG1 functions downstream of EDS1 to regulate TIR-NLR-mediated plant immunity in. Proc Natl Acad Sci U S A 115:E10979-E10987.
Google Scholar: Author Only Title Only Author and Title

Rathjen, J.P., and Dodds, P.N. (2017). Dancing with the Stars: An Asterid NLR Family. Trends Plant Sci 22:1003-1005.
Google Scholar: Author Only Title Only Author and Title

Rietz, S., Stamm, A., Malonek, S., Wagner, S., Becker, D., Medina-Escobar, N., Vlot, A.C., Feys, B.J., Niefind, K., and Parker, J.E. (2011). Different roles of Enhanced Disease Susceptibility1 (EDS1) bound to and dissociated from Phytoalexin Deficient4 (PAD4) in Arabidopsis immunity. New Phytol 191:107-119.
Google Scholar: Author Only Title Only Author and Title

Roberts, M., Tang, S., Stallmann, A., Dangl, J.L., and Bonardi, V. (2013). Genetic requirements for signaling from an autoactive plant NB-LRR intracellular innate immune receptor. PLoS Genet 9:e1003465.
Google Scholar: Author Only Title Only Author and Title

Saile, S.C., Jacob, P., Castel, B., Jubic, L.M., Salas-Gonzáles, I., Bäcker, M., Jones, J.D.G., Dangl, J.L., and El Kasmi, F. (2020). Two unequally redundant "helper" immune receptor families mediate Arabidopsis thaliana intracellular "sensor" immune receptor functions. PLoS Biol 18:e3000783.
Google Scholar: Author Only Title Only Author and Title

Saucet, S.B., Ma, Y., Sarris, P.F., Furzer, O.J., Sohn, K.H., and Jones, J.D. (2015). Two linked pairs of Arabidopsis TNL resistance genes independently confer recognition of bacterial effector AvrRps4. Nat Commun 6:6338.
Google Scholar: Author Only Title Only Author and Title

Schultink, A., Qi, T., Lee, A., Steinbrenner, A.D., and Staskawicz, B. (2017). Roq1 mediates recognition of the Xanthomonas and Pseudomonas effector proteins XopQ and HopQ1. Plant J 92:787-795.
Google Scholar: Author Only Title Only Author and Title

Serra, H., Choi, K., Zhao, X., Blackwell, A.R., Kim, J., and Henderson, I.R. (2018). Interhomolog polymorphism shapes meiotic crossover within the Arabidopsis RAC1 and RPP13 disease resistance genes. PLoS Genet 14:e1007843.
Google Scholar: Author Only Title Only Author and Title

Shao, Z.Q., Xue, J.Y., Wu, P., Zhang, Y.M., Wu, Y., Hang, Y.Y., Wang, B., and Chen, J.Q. (2016). Large-Scale Analyses of Angiosperm Nucleotide-Binding Site-Leucine-Rich Repeat Genes Reveal Three Anciently Diverged Classes with Distinct Evolutionary Patterns. Plant Physiol 170:2095-2109.

Google Scholar: Author Only Title Only Author and Title

Tamborski, J., and Krasileva, K.V. (2020). Evolution of Plant NLRs: From Natural History to Precise Modifications. Annu Rev Plant Biol 71:355-378.
Google Scholar: Author Only Title Only Author and Title

Tan, X., Meyers, B.C., Kozik, A., West, M.A., Morgante, M., St Clair, D.A., Bent, A.F., and Michelmore, R.W. (2007). Global expression analysis of nucleotide binding site-leucine rich repeat-encoding and related genes in Arabidopsis. BMC Plant Biol 7:56.
Google Scholar: Author Only Title Only Author and Title

Thomas, W.J., Thireault, C.A., Kimbrel, J.A., and Chang, J.H. (2009). Recombineering and stable integration of the Pseudomonas syringae pv. syringae 61 hrp/hrc cluster into the genome of the soil bacterium Pseudomonas fluorescens Pf0-1. Plant J 60:919-928.
Google Scholar: Author Only Title Only Author and Title

Tian, L., and Li, X. (2020). Enzyme formation by immune receptors. Science 370:1163-1164.
Google Scholar: Author Only Title Only Author and Title

Tong, M., Kotur, T., Liang, W., Vogelmann, K., Kleine, T., Leister, D., Brieske, C., Yang, S., Lüdke, D., Wiermer, M., et al. (2017). E3 ligase SAUL1 serves as a positive regulator of PAMP-triggered immunity and its homeostasis is monitored by immune receptor SOC3. New Phytol 215:1516-1532.
Google Scholar: Author Only Title Only Author and Title

Van de Weyer, A.L., Monteiro, F., Furzer, O.J., Nishimura, M.T., Cevik, V., Witek, K., Jones, J.D.G., Dangl, J.L., Weigel, D., and Bemm, F. (2019). A Species-Wide Inventory of NLR Genes and Alleles in Arabidopsis thaliana. Cell 178:1260-1272.e1214.
Google Scholar: Author Only Title Only Author and Title

van Wersch, S., and Li, X. (2019). Stronger When Together: Clustering of Plant NLR Disease resistance Genes. Trends Plant Sci 24:688-699.
Google Scholar: Author Only Title Only Author and Title

Wan, L., Essuman, K., Anderson, R.G., Sasaki, Y., Monteiro, F., Chung, E.H., Osborne Nishimura, E., DiAntonio, A., Milbrandt, J., Dangl, J.L., et al. (2019). TIR domains of plant immune receptors are NAD. Science 365:799-803.
Google Scholar: Author Only Title Only Author and Title

Wang, Y., Zhang, Y., Wang, Z., Zhang, X., and Yang, S. (2013). A missense mutation in CHS1, a TIR-NB protein, induces chilling sensitivity in Arabidopsis. Plant J 75:553-565.
Google Scholar: Author Only Title Only Author and Title

Wang, Z.P., Xing, H.L., Dong, L., Zhang, H.Y., Han, C.Y., Wang, X.C., and Chen, Q.J. (2015). Egg cell-specific promoter-controlled CRISPR/Cas9 efficiently generates homozygous mutants for multiple target genes in Arabidopsis in a single generation. Genome Biol 16:144.
Google Scholar: Author Only Title Only Author and Title

Wells, C.A., Chalk, A.M., Forrest, A., Taylor, D., Waddell, N., Schroder, K., Himes, S.R., Faulkner, G., Lo, S., Kasukawa, T., et al. (2006). Alternate transcription of the Toll-like receptor signaling cascade. Genome Biol 7:R10.
Google Scholar: Author Only Title Only Author and Title

Wicker, T., Yahiaoui, N., and Keller, B. (2007). Illegitimate recombination is a major evolutionary mechanism for initiating size variation in plant resistance genes. Plant J 51:631-641.
Google Scholar: Author Only Title Only Author and Title

Wu, C.H., Abd-El-Haliem, A., Bozkurt, T.O., Belhaj, K., Terauchi, R., Vossen, J.H., and Kamoun, S. (2017a). NLR network mediates immunity to diverse plant pathogens. Proc Natl Acad Sci U S A 114:8113-8118.
Google Scholar: Author Only Title Only Author and Title

Wu, C.H., Belhaj, K., Bozkurt, T.O., Birk, M.S., and Kamoun, S. (2016). Helper NLR proteins NRC2a/b and NRC3 but not NRC1 are required for Pto-mediated cell death and resistance in Nicotiana benthamiana. New Phytol 209:1344-1352.
Google Scholar: Author Only Title Only Author and Title

Wu, Z., Huang, S., Zhang, X., Wu, D., Xia, S., and Li, X. (2017b). Regulation of plant immune receptor accumulation through translational repression by a glycine-tyrosine-phenylalanine (GYF) domain protein. Elife 6.
Google Scholar: Author Only Title Only Author and Title

Wu, Z., Li, M., Dong, O.X., Xia, S., Liang, W., Bao, Y., Wasteneys, G., and Li, X. (2019). Differential regulation of TNL-mediated immune signaling by redundant helper CNLs. New Phytol 222:938-953.
Google Scholar: Author Only Title Only Author and Title

Wu, Z., Tong, M., Tian, L., Zhu, C., Liu, X., Zhang, Y., and Li, X. (2020). Plant E3 ligases SNIPER1 and SNIPER2 broadly regulate the homeostasis of sensor NLR immune receptors. EMBO J 39:e104915.
Google Scholar: Author Only Title Only Author and Title

Xu, F., Zhu, C., Cevik, V., Johnson, K., Liu, Y., Sohn, K., Jones, J.D., Holub, E.B., and Li, X. (2015). Autoimmunity conferred by chs3-2D relies on CSA1, its adjacent TNL-encoding neighbour. Sci Rep 5:8792.
Google Scholar: Author Only Title Only Author and Title

Yang, S., Zhang, X., Yue, J.X., Tian, D., and Chen, J.Q. (2008). Recent duplications dominate NBS-encoding gene expansion in two woody species. Mol Genet Genomics 280:187-198.
Google Scholar: Author Only Title Only Author and Title

Zbierzak, A.M., Porfirova, S., Griebel, T., Melzer, M., Parker, J.E., and Dörmann, P. (2013). A TIR-NBS protein encoded by Arabidopsis Chilling Sensitive 1 (CHS1) limits chloroplast damage and cell death at low temperature. Plant J 75:539-552.
Google Scholar: Author Only Title Only Author and Title

Zhang, Y., Song, G., Lal, N.K., Nagalakshmi, U., Li, Y., Zheng, W., Huang, P.J., Branon, T.C., Ting, A.Y., Walley, J.W., et al. (2019). TurboID-based proximity labeling reveals that UBR7 is a regulator of N NLR immune receptor-mediated immunity. Nat Commun 10:3252.
Google Scholar: Author Only Title Only Author and Title

Zhang, Y., Wang, Y., Liu, J., Ding, Y., Wang, S., Zhang, X., Liu, Y., and Yang, S. (2017). Temperature-dependent autoimmunity mediated by chs1 requires its neighboring TNL gene SOC3. New Phytol 213:1330-1345.
Google Scholar: Author Only Title Only Author and Title

Zhao, T., Rui, L., Li, J., Nishimura, M.T., Vogel, J.P., Liu, N., Liu, S., Zhao, Y., Dangl, J.L., and Tang, D. (2015). A truncated NLR protein, TIR-NBS2, is required for activated defense responses in the exo70B1 mutant. PLoS Genet 11:e1004945.
Google Scholar: Author Only Title Only Author and Title

Zhong, Y., and Cheng, Z.M. (2016). A unique RPW8-encoding class of genes that originated in early land plants and evolved through domain fission, fusion, and duplication. Sci Rep 6:32923.
Google Scholar: Author Only Title Only Author and Title